

Synthesis and study of dielectric and magnetic properties of aluminum lithium and nickel doped strontium hexaferrites nanoparticles.



Submitted By

Tania Afzal

School of Chemical and Materials Engineering (SCME)

National University of Sciences and Technology (NUST)

2022

Synthesis and study of dielectric and magnetic properties of aluminum lithium and nickel doped strontium hexaferrites nanoparticles.



Name: Tania Afzal

Registration No: 00000275451

This thesis is submitted as a partial fulfillment of the requirement for the degree of

MS in Nano science and Engineering

Supervisor Name: Dr.Usman Liaqat

School of Chemical and Materials Engineering (SCME)

National University of Sciences and Technology (NUST)

Certificate

This is to certify that work in this thesis has been carried out by **Miss Tania Afzal** and completed under my supervision in Thermal Transport Laboratory at School of Chemical and Materials Engineering, National University of Sciences and Technology, H-12, Islamabad, Pakistan.

Supervisor: _____

Dr. Usman Liaqat

Materials Engineering, Department

National University of Sciences

and Technology, Islamabad.

Submitted through _____

Principal/Dean,

School of Chemicals and Materials Engineering Department

National University of Sciences and Technology, Islamabad.

Dedication

I would like to dedicate this thesis to my beloved parents and teachers for their continuous support, patience and faith upon me.

Acknowledgements

“Truly my prayer, my service of sacrifice, my life and my death are all for Allah, the lord of worlds.”

First of all acknowledgement goes to Allah Almighty Who granted me the wisdom and passion to execute my work.

Secondly, I am privileged to express gratitude to Principal (SCME NUST) to my supervisor Dr. Usman Liaqat and my committee members Dr. I.H Gul and Dr. Aftab Akram for their support and advice at every stage of research work.

At last, but not the least, I acknowledge all the family members, non-teaching staff and research colleagues Fatima Ishaq, Majida Chaudhry, Hadiqa kiyani and Asia nisar who supported me throughout my research work.

Sincerely,

Tania Afzal Khan.

Abstract

In the present study synthesis of strontium hexaferrites with chemical compositions $\text{SrFe}_{12}\text{O}_{19}$ and $\text{SrFe}_{12-2x}(\text{Al}, \text{Li}, \text{Ni})_x\text{O}_{19}$ was performed by sol gel method. Initially pure strontium hexaferrites with chemical composition $\text{SrFe}_{12}\text{O}_{19}$ was synthesized and then doped strontium hexaferrites with chemical composition $\text{SrFe}_{12-2x}(\text{Al}, \text{Li}, \text{Ni})_x\text{O}_{19}$ was synthesized with variation in dopants' concentration from $x=0, 0.2, 0.35$ and 0.5 . Stoichiometric amount of strontium, iron, aluminum, lithium nickel nitrates and citric acid along with ammonia solution to maintain pH of solution were used to prepare sample. The characterization was performed using X-ray diffraction technique and Fourier transform infrared spectroscopy. The electrical properties were examined by using RF Impedance analyzer and magnetic properties were examined using Vibrating sample magnetometer. Crystallite size was calculated by Debye Scherrer formula which came out in the range of 27nm to 35nm. By dielectric properties measurement an increase in dielectric constant, dielectric loss and tangent at low frequency and started to decrease at higher frequencies and eventually became constant. This effect had been correlated to the impact of grain boundaries at low and high frequency. Magnetic properties measurement was performed by using vibrating sample magnetometer that revealed that the saturation magnetization decreased with the increase in dopants' concentration due to accumulation of cations at interstitial sites with upward spin. Coercivity also decreased with increasing dopant concentration giving rise to the impact that the material is moving towards being softer.

Table of Contents

Chapter 1.....	1
Introduction	1
1.1 Ferrites	1
1.1.1 History of Ferrites.....	1
1.2 History of Magnetism:.....	2
1.2.1 Diamagnetism:.....	2
1.2.2 Para magnetism:	3
1.2.3 Ferromagnetism:.....	4
1.2.4 Antiferromagnetism:.....	5
1.2.5 Ferrimagnetism:.....	6
1.2.6 Soft Ferrites:	7
1.2.7 Hard Ferrites:	7
1.3 Classification of Ferrites:.....	7
1.3.1 Spinal Ferrites:.....	8
1.3.2 Garnet Ferrites:	9
1.3.3 Ortho Ferrites.....	9
1.3.4 Hexagonal Ferrites:.....	10
1.4 Crystal Structure:.....	10
1.5 Properties Of hexaferrites:.....	11
1.5.1 Dielectric Properties:	11
1.5.2 Magnetic Properties:.....	11
1.5.3 Physical Properties:	12
1.5.4 Photocatalytic Properties:.....	12
1.6 Significance of Ferrites:.....	12
1.7 Few of the recent applications of ferrites are listed below:	13
Chapter 2.....	14
Literature Review	14
Chapter 3.....	19
Synthesis.....	19
3.1 Synthesis of Nanoparticles:	19
3.1.1 Classification of the techniques for the synthesis of nanomaterials:	19

3.1.2 Top down Approach:	20
3.1.3 Bottom-up Approach:	20
3.2 Sol Gel Technique:	22
3.2.1 Sol gel process steps:	23
3.2.2 Homogeneous solution formation:	23
Sol Formation:	24
3.2.3 Gelation:	24
3.2.4 Advantages:	24
3.3 Experimental Procedure:	24
3.4 Synthesis of SrFe _{12-2x} (Al, Li, Ni) _x O ₁₉	25
3.5 Synthesis of Aluminum, lithium and Nickel doped Strontium hexaferrites:	26
Chapter 4.....	27
Characterization Techniques	27
4.1 X-ray diffraction Technique:	27
4.1.1 Working of XRD:	27
4.1.2 Powder Diffraction Method:.....	29
4.1.3 Lattice Constant:.....	29
4.1.4 Crystallite Size:.....	30
4.2 Fourier transform infrared Spectroscopy:.....	30
4.2.1 Basic principle of FTIR:	31
4.2.2 Instrumentation:	32
4.3 Dielectric:	33
4.3.1 Dipolar and Orientation Polarization:.....	34
4.3.2 Ionic Polarization:.....	34
4.3.3 Interface and space charge Polarization:	35
4.3.4 Electronic and Atomic Polarization:.....	35
4.4 Vibrating Sample Magnetometry:	36
4.4.1 Working Principle:	36
4.4.2 Instrumentation:.....	36
Chapter 5.....	38
Results and Discussion:	38
5.1 XRD Analysis:.....	38

5.1.1 Strontium Hexaferrite doped with Al, Li, Ni [SrFe _{12-2x} (Al, Li, Ni) O ₁₉]:	39
5.2 Ftir:	41
5.3 Dielectric Constant:	43
5.4 Dielectric Loss:	45
5.5 Tangent Loss:	47
AC Conductivity:.....	50
5.6 VSM:	52
Conclusion:	55
Future Work.....	56

List of Figures:

Figure 1 : Atomic dipoles Alignment in Diamagnetic Materials.....	3
Figure 2: Atomic dipoles Alignment In Paramagnetic Materials	4
Figure 3: Atomic dipoles Alignment in Ferromagnetic Materials.....	5
Figure 4: Atomic Dipoles Alignment in Anti-ferromagnetic Materials	6
Figure 5: Alignment of Atomic Dipoles in Ferromagnetic Materials.....	6
Figure 6: FCC Cubic unit cell of Spinal Ferrites	8
Figure 7: Representation of crystal structure of Garnet Ferrites:	9
Figure 8: Representation of crystal structure of Ortho ferrites	10
Figure 9: Representation of crystal structure of hexagonal Ferrites	11
Figure 10: Representation of top down Approach.....	19
Figure 11: Representation of top down Approach.....	20
Figure 12: Representation of bottom up Approach.....	21
Figure 13: Schematic of Sol gel method for nanoparticles Fabrication.....	23
Figure 14: Schematic of synthesis of strontium ferrites by Sol gel method	26
Figure 15: Scattering of Incident X-ray by a plane.....	28
Figure 16: X ray Diffraction	29
Figure 17: Schematic figure of FTIR.....	32
Figure 18: Impedance Analyzer.....	33
Figure 19: Dipolar Polarization	34
Figure 20: Ionic Polarization	35
Figure 21: Space Charge Polarization.....	35
Figure 22: Electronic Polarization	36
Figure 23: Schematic of VSM	37
Figure 24: XRD pattern of pure strontium hexaferrites.....	38
Figure 25 : XRD pattern of doped strontium hexaferrites	39
Figure 26: FTIR Spectrum.....	42
Figure 27: Dielectric Constant Variation with frequency.....	44
Figure 28: Dielectric loss variation with Frequency.....	46
Figure 29 : Tangent loss variation with Frequency	48

Figure 30: Hysteresis loop for pure and doped strontium ferrites53

List of Tables

Table 1: Lattice Parameters and crystallite size of pure and doped strontium hexaferrites	40
Table 2: Dielectric constant of pure and doped strontium hexaferrites	45
Table 3: Dielectric loss of pure and doped strontium hexaferrites	47
Table 4: Tangent loss of pure and doped strontium hexaferrites	49
Table 5: Ac conductivity plot for pure and doped strontium hexaferrites	51
Table 7: Values of saturation magnetization, remanence and coercivity for pure and doped strontium ferrites	54

Chapter 1

Introduction

The latest technology has led to the evolution of the economy from agricultural based system to the information based system. As a result, it changed the social structure and living ways of individuals. Being a social member scientist must keep pace with this growing technology. A lot of information is revealed daily which need to be managed effectively. Long ago the discovery of stones led the history of ferrites. Ferromagnetic materials became an innovative research tool for fast growing research technology since long ago. Ferrites particularly hexagonal ferrites are excellent materials for variety of applications due to their low cost and easy manufacturing ways.

1.1 Ferrites

Magnetic materials peculiarly ferrites have achieved a lot of keen interest in research era of science and technology due to their vast applications in abundant fields. Ferrimagnetic materials having proper proportions of metal oxides and iron oxides are known as ferrites. They own twin properties of magnetic conductor and electric insulator. [1] They are hard, brittle, and grey in colour. The magnetic and electric properties possessed by ferrites are high electrical resistivity, high magneto-crystalline anisotropy, low eddy currents and dielectric losses, high Curie temperature and high saturation magnetization. Presence of these properties has increased the successful use of ferrites in different applications like antenna rods, transformer cores and magnetic storage devices, permanent magnets, and magnetic resonance imaging.

....

1.1.1 History of Ferrites

The word ferrite came from a Latin word **ferrum** that means iron. The history of ferrites begun with the discovery of an iron oxide magnetic material known as load stone (Fe_3O_4) which was originally found in Asia slight and then termed as ferrite. The magnetic

properties of magnetite then observed by ancient Chinese. Later, in 1600 these magnetic properties were further described by William Gilbert and then published in first book of magnetism entitled “De Magnate”. Magnetism and electricity were also differentiated by the William Gilbert and paid a great contribution in the discovery of earth magnetic field.[2]

1.2 History of Magnetism:

In early centuries the term magnetism was originally derived from the word magnesia that is an Aegean Sea Island in other words the land of stones. The spin and orbital motion as well as in between interactions of electrons described the phenomenon of magnetism. A magnetic moment corresponds to both spin and orbital motion of the unpaired electrons. Movement of charge generates magnetic field. The ability of a material to respond towards magnetic field is magnetism.[3]’ The magnetic behavior of the materials classifies them into five different groups

Diamagnetism

Para-magnetism

Ferromagnetism

Ferrimagnetism

Antiferromagnetism

1.2.1 Diamagnetism:

This phenomenon of magnetism exists in class of materials that have no net magnetic moment. Since electrons revolve around the nucleus in their orbits and produce a magnetic field around themselves. These materials when subjected to an external applied field then they oppose that field by the field produced by orbital motion of electrons and hence cancel the effect of each other.[4] Thus, diamagnetic materials when exposed to an external magnetic field generate magnetic field and temperature independent negative susceptibility. When external field is removed this material cannot retain their magnetization. [5]

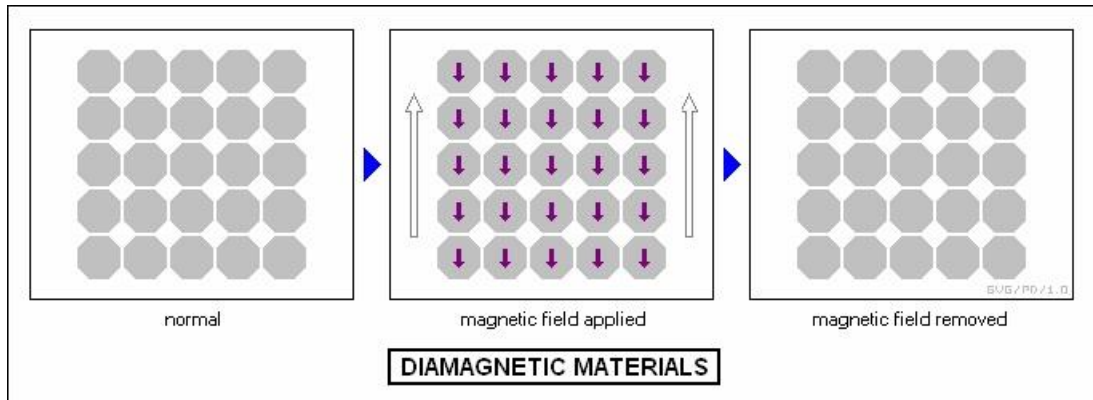


Figure 1 : Atomic dipoles Alignment in Diamagnetic Materials

1.2.2 Para magnetism:

In Para magnetic materials the magnetic moments do not cancel the effect of each other. The magnetic moments are used to be randomly oriented in the absence of magnetic field and have no net macroscopic magnetization. When these types of materials are subjected to an external field then the magnetic dipole moments undergo a regular alignment in the direction of the applied field and then have a net magnetization and lead to a positive susceptibility. Unlike to diamagnetic materials Para magnetism phenomenon in materials would subject them to have temperature dependent susceptibility. [6-7]

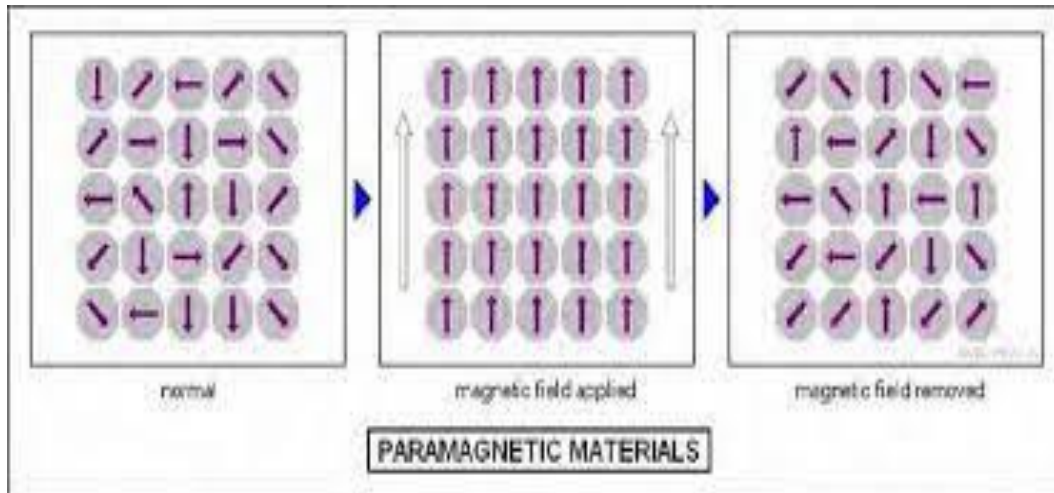


Figure 2: Atomic dipoles Alignment in Paramagnetic Materials

1.2.3 Ferromagnetism:

The class of magnetic materials that have permanent high atomic moments even when there is no magnetic field applied. These materials exhibit strong high interactions and result in parallel alignment of magnetic moments with neighboring atoms and have large net magnetization. They have high magnetic permeability and are capable to have permanent magnetization in absence of external applied field. The atoms present in these materials undergo quantum mechanical exchange interactions between them and then result in the regions having permanent magnetization. Regions where all the magnetic moments are aligned in the same direction. Ferromagnetic behavior occurs below a certain temperature called as Curie temperature above this temperature materials loses its own behavior and becomes paramagnetic.[8]

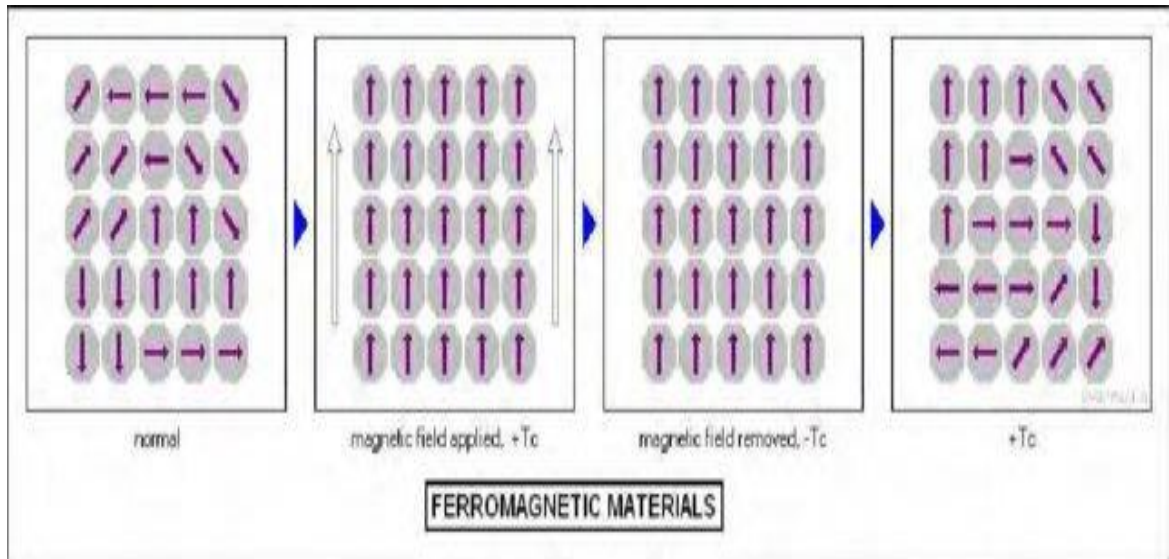


Figure 3: Atomic dipoles Alignment in Ferromagnetic Materials

1.2.4 Antiferromagnetism:

In this phenomenon the magnetic dipole moments of adjacent atoms are anti-parallel to each other and hold no net magnetic moment. This anti-parallel alignment comes because of the quantum mechanical exchange interactions of atoms with neighboring atoms. In anti-ferromagnetic materials in contrast to ferromagnetic there is no net magnetization in the absence of field. This magnetic behavior occurs below a critical temperature called Neel temperature.[9] Likewise ferromagnetic above this temperature the material becomes paramagnetic.

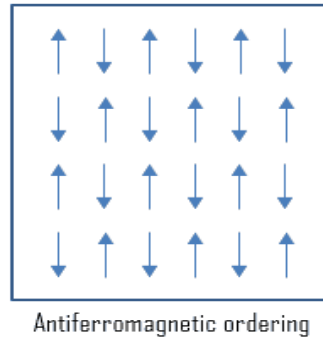


Figure 4: Atomic Dipoles Alignment in Anti-ferromagnetic Materials

1.2.5 Ferrimagnetism:

The ferromagnetic behavior is almost like ferromagnetic behavior below Curie temperature. The magnetic moments in these materials are aligned anti parallel to each other but have different magnitude and magnetic moment of one atom is greater than the oppositely aligned magnetic moment of other atom and hence do not cancel the effect of each other resulting into net magnetization. These magnetic materials do not lose their magnetization although if there is no external applied field.[10] Ferrimagnetic materials are basically non-conducting and have no eddy current losses.

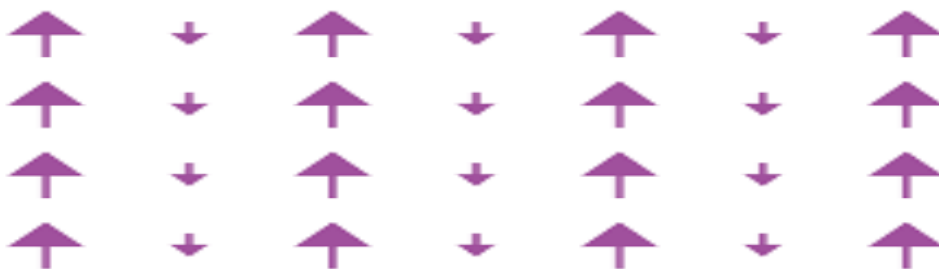


Figure 5: Alignment of Atomic Dipoles in Ferromagnetic Materials

In accordance to the magnetic nature of the magnetic materials there are further classified into two categories such soft ferrites and hard ferrites.

1.2.6 Soft Ferrites:

Ferrimagnetic materials that cannot hold on to their magnetism for so long after being magnetized are known as soft ferrites. These materials have cubic crystal structure MFe_2O_4 here M represents the distribution of cations like Ni, Zn etc. Soft ferrites form steeply rising magnetization curve forming small and narrow B-H hysteresis loop and have low coercivity values as well as attain high susceptibility. It is better to heat and then slowly cooling these materials can be helpful in the formulation of these materials. Due to low coercivity values soft ferrites can be easily magnetized and demagnetized.[11]

1.2.7 Hard Ferrites:

Magnetic materials that can retain their magnetism even for so long when they are magnetized are known as hard ferrites also called as permanent magnets. These materials undergo slowly rising magnetization curve, large energy losses and form broad B-H hysteresis loop. Hard ferrites as per their name suggests cannot be easily magnetized and demagnetized. Heating and sudden cooling based process can be helpful in the formulation of these type of materials. Hard ferrites exhibit high coercivity values, high eddy current losses, high saturation magnetization, low susceptibility, and permeability.[12]

1.3 Classification of Ferrites:

Based on composition and crystal structure of ferrimagnetic ferrites are further classified into four main types:

Spinal Ferrites

Garnet Ferrites

Ortho Ferrites

Hexagonal Ferrites

1.3.1 Spinal Ferrites:

The class of materials with chemical composition AB_2O_4 where A can be Fe, Mg, Zn, Mn, Ni etc. and B can be Al, Fe or Cr are termed as spinal ferrites. Spinal ferrites have face centered cubic crystal structure with A and B as divalent trivalent or tetravalent cations and oxides as anions. This structure describes the unit cell having 8 divalent metal ions, 16 trivalent metal ions and 32 oxygen ions that further discloses two types of interstices possibly filled by metal ions. The interstices are named as tetrahedral A sites and octahedral B sites. The tetrahedral sites have cations magnetic moments aligned in the same direction but are anti-parallel to those of octahedral sites.[13]

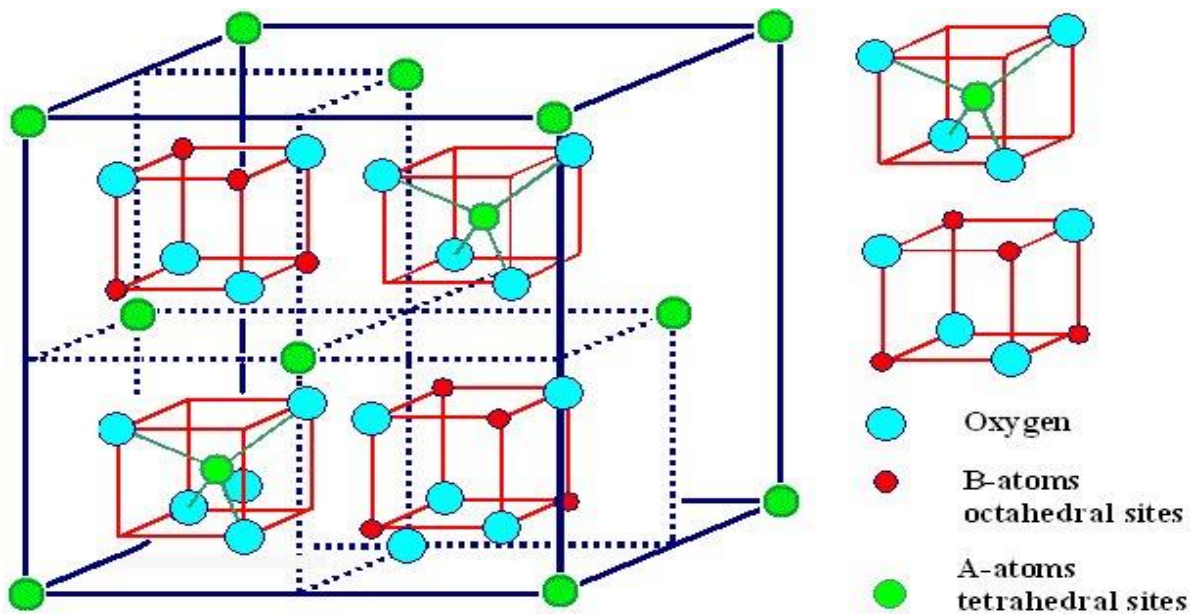


Figure 6: FCC Cubic unit cell of Spinal Ferrites

Spinal Ferrites possess insulating and magnetic characteristics. These are soft ferrites and is readily magnetically reversible. Spinal Ferrites bear moderate coercivity values and low eddy current losses and strong electrical resistance. Being soft ferrites, they have low saturation magnetization. Spinal ferrites have multiple uses in various applications like

transformer cores, magnetic resonance imaging, for drug delivery and in radio frequency applications etc. [14]

1.3.2 Garnet Ferrites:

These types of ferrites are mostly useful for high frequency applications, nano fluids, magnetic refrigerators, electromagnetic shielding materials and in electromagnetic absorption processes. Owing to difference in crystal structure second type of ferrites is garnet ferrites. These types of ferrites have crystal structure formula $\text{Me}_3\text{B}_5\text{O}_{12}$, here Me is rare earth trivalent ion, B represents transition metal cation and X belongs to any anionic specie usually oxygen. The crystal structure of Garnet composed of A tetrahedral sites B octahedral sites and C dodecahedral sites. Iron cations are distributed at tetrahedral and octahedral sites whereas Me cations occupy dodecahedral sites. Garnet ferrites are well known optically transparent materials.[15]

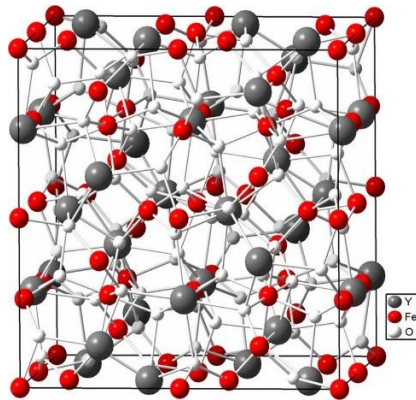


Figure 7: Representation of crystal structure of Garnet Ferrites:

1.3.3 Ortho Ferrites

Materials holding perovskite structure ABX_3 here A is alkaline metal cation, B is transition metal cation and X is anionic specie usually oxygen. Iron being the central ion forms an octahedra. The interstitial sites are occupied by alkaline cations surrounded by oxygen atoms. They exhibit weak ferromagnetism. Orthoferrites are usually used in magnetic field sensors for their high domain wall velocity also used in communication techniques.

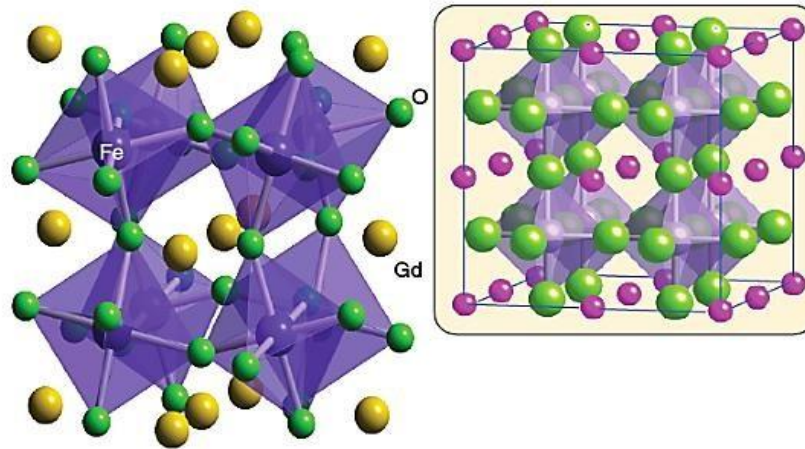


Figure 8: Representation of crystal structure of Ortho ferrites

1.3.4 Hexagonal Ferrites:

Hexagonal ferrites were initially discovered in 1950's and then became covered a huge era of research. Being fourth group ferrite materials, they are further classified into five types each with different chemical composition and formula such as M, U, W, X, Y and Z. These materials hold chemical formula $\text{MeFe}_{12}\text{O}_{19}$ where Me represents divalent ion such as Sr, Ba and Pb. Hexaferrites having strontium barium and calcium as main constituent with iron attain high coercivity, permeability and conduct magnetic flux as well. Hexagonal ferrites got huge attention in electronic industry due to their remarkable electric and magnetic properties and low manufacturing cost.[16]

1.4 Crystal Structure:

Hexagonal ferrites with chemical formula $\text{MeFe}_{12}\text{O}_{19}$ there is closely packed oxygen ions layer and the incorporation of divalent and trivalent metal ions takes place in interstices. In crystal structure there are three S, R and T blocks rotating at 180° around c axis. When subunit R combines with S^{+2} a neutral RS block with $\text{MFe}_{12}\text{O}_{19}$ is formed. Likewise, when T subunit combines with S^0 a neutral TS block will form named as Y block. Similarly, upon stacking sequence variation of hexagonal and cubic units different compositions can be formed.

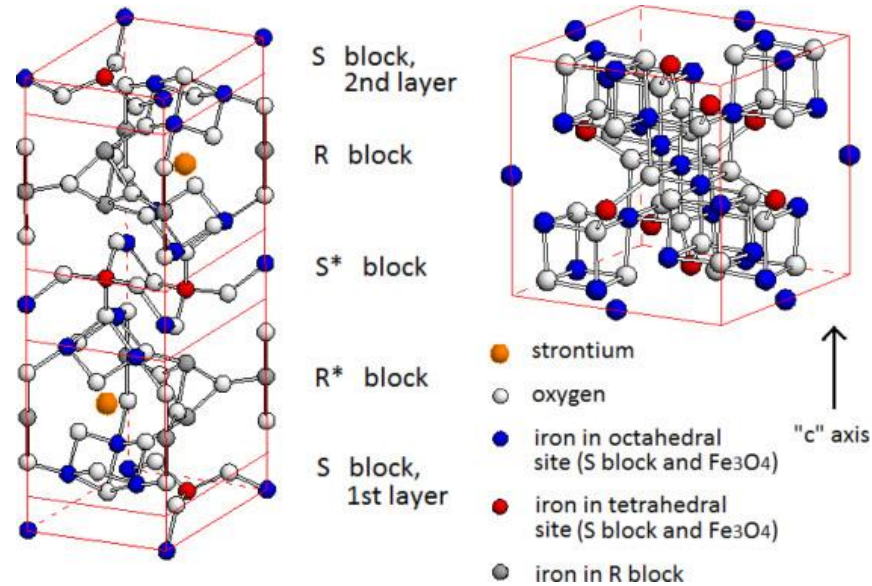


Figure 9: Representation of crystal structure of hexagonal Ferrites

1.5 Properties Of hexaferrites:

Depending upon the nature and composition hexaferrites exhibit various physical, magnetic, dielectric and photocatalytic properties few of them are as follows:

1.5.1 Dielectric Properties:

Various attributes like dielectric loss, dielectric constant, tangent loss and ac conductivity and elastic modulus are included in dielectric properties of ferrites. These attributes may vary with changing composition of the materials. Dielectric properties primarily provide detail regarding the formulation of electric field in the material.[12]

1.5.2 Magnetic Properties:

Magnetic properties of ferrites include saturation magnetization, magnetic coercivity and remanence. They alter by varying the composition of materials through doping of different metal cations like aluminum, nickel etc. The size of the crystal varies in large cations like strontium barium that become the source of magnetic anisotropy and subsequently alter the magnetic properties.

The XRD pattern of hexaferrites differs from other ferrites that's why their magnetization is usually shown in c-axis. For the fabrication of microelectronics, ferrites are synthesized at higher temperature of around 900°C. [13]

1.5.3 Physical Properties:

Physical properties of ferrite nanoparticles depend upon composition. Composition change produces significant change in physical properties. Ferrites that possess strong physical properties and being excellently hard are used for making permanent magnets.

For the fabrication of microelectronics, ferrites are synthesized at higher temperature of around 900°C. [18]

1.5.4 Photocatalytic Properties:

Photocatalysis of visible light is more suitable with ferrites since their band gap lies in visible region. Ferrites are usually used for the degradation of synthetic dyes. Hexaferrites possess high saturation magnetization, coercivity and thermal stability so when added with hydrogen peroxide a Photon Fenton type degradation occurs.[16]

1.6 Significance of Ferrites:

Ferrites are considered as very important magnetic materials for their easy manufacturing, low cost and strong magnetic properties.[17] They are widely used due to having following properties:

Low eddy losses

Cheap to assemble

High saturation magnetization

High resistivity

High coercivity of specific ferrites

Mechanical stiffness

Useful time and temperature stability

High permeability

1.7 Few of the recent applications of ferrites are listed below:

In drug delivery and pesticide delivery

In magnetic recording media

In chokes and transformers

Used in electrode manufacturing for chromium plating

In magnetic sensors

High frequency applications

For magnetic shielding

Objective of the Research

The objectives of the research are as follows:

Synthesis of strontium hexaferrite with chemical composition $\text{SrFe}_{12}\text{O}_{19}$ by sol gel method.

Synthesis of doped strontium hexaferrite with chemical composition $\text{SrFe}_{12-2x}(\text{Al}, \text{Li Ni})_x\text{O}_{19}$ by sol gel method.

Study of structural, electrical and magnetic properties at different concentration of dopants.

To investigate the effect of Al, Li and Ni doping on electrical and magnetic properties of the strontium hexaferrites.

Chapter 2

Literature Review

[19]. synthesized strontium hexaferrites nanoparticles $\text{SrFe}_{12-x}\text{Al}_x\text{O}_{19}$ doped with aluminum through auto combustion method. Formation of M phase ferrites successfully revealed through x-ray diffraction technique. With the increase in Al^{3+} doping content a decrease in lattice parameter has been observed. Transmission electron microscopy techniques was being used for morphological analysis of the samples. Magnetic behavior change had been observed at different doping levels of aluminum. Particles had shown ferromagnetic and ferrimagnetic trend at low doping level of aluminum at $x < 4$ and at high doping level i.e. $x > 4$. The coercivity values had been increased first at low doping level of Al^{3+} and then decreased at high doping content of Al^{3+} . This behavior has been related to magneto crystalline anisotropy and size of the particles.

[20]. sol gel combustion method was being used to synthesize the doped strontium hexaferrites with chemical composition as $\text{Sr}_{1-x}\text{Dy}_x\text{Fe}_{12-y}\text{Ni}_y\text{O}_{19}$ with Dy and Ni as doping contents. M type hexagonal structure of the synthesized samples was confirmed through XRD analysis. The average particle size of 40-50nm measured through SEM that further revealed the spherical and hexagonal structure of particles. The dielectric and magnetic properties analysis was performed. A certain increase in the saturation magnetization, remanence and coercivity had been observed. Due to this increase materials were recommended for high density recording media applications. Furthermore, dc resistivity increment and falling off in dielectric loss related these materials useful for applications in microwave devices.

[22]. doped strontium hexaferrites were prepared through solid state reaction method. Structural analysis was performed through x-ray diffraction technique. A decrease in grain size was detected up to micron. SiO_2 strongly affected the structural, morphological electrical and magnetic properties of Sr hexaferrites. With the substitution of silica decrease in remanence and increase in coercivity was investigated. The dc resistivity increased that suggested these materials useful for magnetic applications that require high resistivity. In

dielectric properties measurement it had been observed that the dielectric constant and dielectric loss remained in 3340-12 and 5.75-0.21 from 80Hz to 1MHz frequency range.

[23].The M type hexaferrites were investigated with the addition of nickel and cobalt. The barium strontium hexaferrites materials with general formula $\text{Ba}_{0.5}\text{Sr}_{0.5}\text{Ni}_x\text{Co}_x\text{Fe}_{12-2x}\text{O}_{19}$ synthesized by sol gel method and then characterization techniques like XRD, SEM and VSM were performed. Structural analysis through XRD confirmed the formation of single magnetoplumbite phase structure bearing materials. The average grain size increased with the substitution of Ni and Co also adding formation of dense structure. A successive decrease in saturation magnetization and coercivity had been observed by the increase in doping concentration. This decrease in magnetization and coercivity became the cause behind to shift towards the soft magnetic materials. The substituted cations occupied at the preferential sites led to the variation in the magnetic properties.

[24].Nickel doped strontium hexaferrites were synthesized through coprecipitation method and structural, morphological, magnetic, and dielectric analysis were performed through various characterization techniques. $\text{SrNi}_x\text{Fe}_{12-2x}\text{O}_{19}$ powder samples prepared by coprecipitation method and then by using usual sintering method were densified at $1100^{\circ}\text{C}/4\text{h}$.Through XRD technique it has revealed that at low doping concentration that is up to $x=0.4$ samples showed no detection any impurity phase but at higher dopant concentration for $x\geq 0.6$ formation of secondary phases was identified. Similarly, a different trend in saturation magnetization at low and high dopant concentration was discovered. MS decreased up to $x=0.6$ and then increased for $x>0.6$. Doping increased coercivity values anisotropic ally. Dielectric constant increased at low frequency and then decreased at higher frequency.

[25]. Sol gel auto combustion method was used to synthesize the nickel doped strontium hexaferrites. Doping effect of nickel on $\text{SrFe}_{12-x}\text{Ni}_x\text{O}_{19}$ was identified through XRD, SEM, FTIR, VSM and dielectric properties measurement. XRD measurement confirmed the formation of single phase strontium hexa ferrites at low doping concentration for $x\leq 0.5$ and showed NiFeO_4 at high doping concentration. The particle size of 49-54nm was identified. By FTIR spectra three absorption peaks were observed that confirmed the existence of iron nickel stretching bands. The saturation magnetization increased with increase in the dopant

concentration up to a certain level and then slowly decreased. This attribute was related to the nickel ion occupation at different lattice sites. On the other hand, coercivity showed a decreasing trend with the increase in dopant concentration and this had been related to the anisotropy constant.

[26]. X type hexagonal strontium barium ferrites were prepared using sol gel route. Dielectric and structural properties were deeply investigated through various characterization techniques analysis like XRD, SEM, FTIR, Dielectric and VSM. Single phase characteristics had been observed in materials those annealed at 1250°C. Lattice parameter displayed increasing trend that was related to the larger radius of Nd^{3+} than Fe^{3+} . Fourier transform infrared spectroscopy analysis determined that the vibrational frequency of Fe-O band got effected at tetrahedral and octahedral sites. Furthermore dielectric properties presented various changes upon addition of dopant materials. Dielectric loss, dielectric constant and ac conductivity had been observed decreasing within increasing amount of dopant contents. Through all characteristic analysis it was concluded that SrBa-Cu X type ferrites can be made useful in reducing dielectric losses and ac conductivity through the incorporation of Nd-Ni.

[27] Synthesis and characterization of lithium nickel ferrites had been performed. Single phase lithium nickel ferrites with chemical formula $\text{Li}_{0.5-0.5x} \text{Ni}_x \text{Fe}_{2.5-0.5x} \text{O}_4$ were prepared through ceramic method. By X-ray diffraction analysis spinal structure was determined. For the whole range of nickel concentration lattice constant found to be almost constant throughout the lattice whether the x-ray density increased. Owing to small amounts of Fe^{2+} ions presence in ferrite, splitting occurred in the absorption band which was indicated by Infrared spectroscopy. Elastic moduli variation had been related to the binding forces present between the atoms in spinal lattice. Moreover, transverse, and longitudinal wave velocities and Debye temperature had also been determined.

[28] M type hexagonal magnetoplumbite ferrites chemical formula $\text{SrFe}_{12-x}\text{Al}_x\text{O}_{19}$ have been prepared by citrate nitrate sol gel method and were profoundly investigated the doping effect of aluminum upon crystal structure, remanence M_r , saturation magnetization by various characterization techniques. XRD analysis confirmed single phase magnetoplumbite structure of the synthesized materials. Within increasing amount of

doping content aluminum, the saturation magnetization and remanence decreased whereas the coercivity showed fluctuation and attained the value of 10.59 kOe at $x=0.5$. Also, it had been concluded that Al substitution changed the intergranular magnetostatic interactions to exchange coupling interactions.

[29] prepared aluminum doped cobalt ferrites $\text{CoAl}_y\text{Fe}_{2-y}\text{O}_4$ by sol gel auto combustion method. Structural analysis and magnetic properties measurement had been done through x-ray diffraction, transmission electron microscopy and vibrating sample microscopy. XRD plots revealed the decrease in grain size and lattice parameter as well as confirmed the formation of single phase spinel ferrites. Since increase in dopant concentration led to the increase in amount of non-magnetic Al^{3+} ions that became the reason of decrease in saturation magnetization and coercivity.

[29] Substitution of Gd in strontium hexaferrites had been examined in two different series of samples such as $(\text{Sr}_{1-x}\text{Gd}_x) \text{O} \cdot 5.25\text{Fe}_2\text{O}_3$ and $\text{Sr}_{1-x}\text{Gd}_x\text{Fe}_{12-x}\text{Co}_x\text{O}_{19}$. Ceramic method had been used for the synthesis of desired particles which then characterized through various techniques. Hexaferrite crystal structure had been observed by XRD analysis. Owing to the magnetic properties remanence and saturation magnetization for Sr-Gd samples remained constant while coercivity increased up to a certain value. On the other hand, coercivity and magnetization for Sr-Gd-Co samples displayed a steady decrease with the substitution.

[30] Study of effect of cobalt substitution in strontium hexa ferrites had been performed. Synthesis of samples with chemical formula $\text{SrAl}_4\text{Fe}_{8-x}\text{Co}_x\text{O}_{19}$ was performed by sol gel method. Hexagonal crystal structure was confirmed by the X-Ray diffraction analysis. Within increase in cobalt concentration the grain size increased. Increased in dopant concentration resulted in decrease of coercivity values while saturation magnetization increased. Dielectric studies displayed regular increase in dielectric constant tangent loss.

[31] Structural and magnetic properties of M type ferrites upon La-Cu substitution had been examined. Nanoparticles of strontium hexaferrites with chemical composition $\text{Sr}_{1-x}\text{La}_x\text{Fe}_{12-x}\text{Cu}_x\text{O}_{19}$ were prepared by self-propagating high temperature synthesis method. XRD analysis confirmed the formation of single Sr M type phase particles. Furthermore, upon the investigation of magnetic properties it had been concluded that there came a remarkable improvement with La-Co substitution.

[32] Coprecipitation method was used to synthesize chromium zinc doped M type strontium hexa ferrites. Doping effect of Cr-Zn on structural, dielectric and magnetic properties had been deeply investigated by using various characterization techniques. By XRD data analysis formation of doped hexaferrites nanoparticles had been confirmed. Using scanning electron microscopy technique, it had been revealed that the Cr-Zn doping dwells grain growth. Dielectric constant and dielectric loss decrement was discovered through dielectric properties measurement that decrease in dielectric loss was then suggested as a cause of Cr-Zn doped strontium ferrites as good promising materials for high frequency applications. It had been found that the coercivity and saturation magnetization were both decreased within growing dopant's concentration.

[33] Single phase M type strontium hexa ferrites were prepared by complex polymerizable method. Diameter range of 20 to 500nm was analyzed by SEM technique. Doping effect of La-Co substitution on magnetic properties was then investigated. It had been examined through vibrating sample magnetometer that by increasing the dopant concentration there come an increase in the coercive force-H loop broadening had been observed proposing the synthesized materials as good hard ferrites.

[34] Calcium strontium hexaferrites doped with copper and zirconium had been examined through various characterization techniques. Coprecipitation method had been used for the synthesis purpose. Single phase hexagonal crystal structure of the synthesized particles was observed through XRD analysis. By measuring dielectric properties, it had been investigated that dielectric constant increased with increasing dopant concentration up to certain value and then decreased. Saturation magnetization found to be decreasing with the increasing impurity concentration. The coercivity also increased earlier up to certain value of dopant amount and then decreased. Synthesized materials were suggested as suitable to be use in high frequency and high density recording media applications.

Chapter 3

Synthesis

3.1 Synthesis of Nanoparticles:

Many techniques have been explored to design nanomaterial having controlled shape, size, structure and dimension. The properties of the materials depend upon the composition, structure as well as defects that are enormously influenced by the kinetics and thermodynamics of the fabrication process.[35]

3.1.1 Classification of the techniques for the synthesis of nanomaterials:

There are basically two types of approaches most probably used to synthesize nanoparticles such as

Top-Down Approach

Bottom-Up Approach

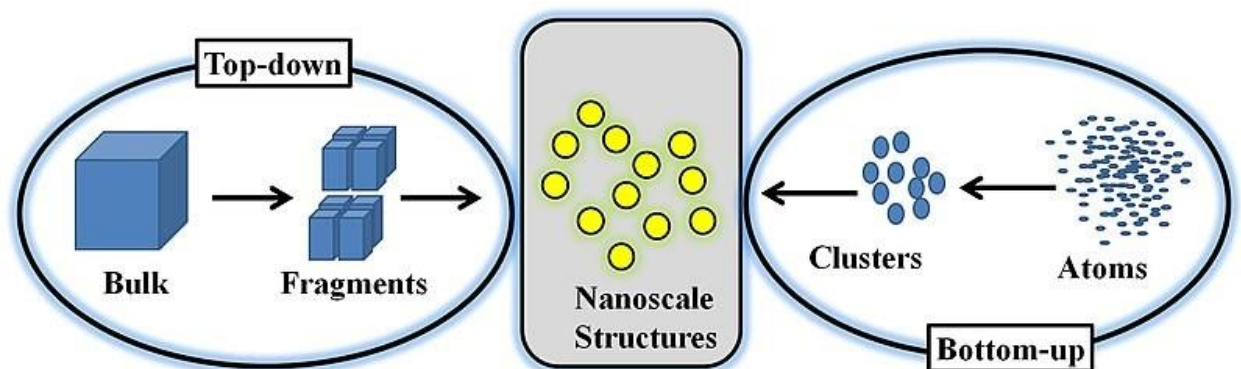


Figure 10: Representation of top down Approach

3.1.2 Top down Approach:

In this approach miniaturization of the bulk materials to nanometer scale is performed. The fabrication procedure involves three steps: modeling, synthesis and optimization. This approach involves lithography, etching, mechanical milling, sputtering and electro explosion. These techniques are assumed as extensions of those have been used for formation of micron sized particles. There are some merits and demerits of this technique like the surface of final product formed by using this technique may accumulate some impurities.[35]

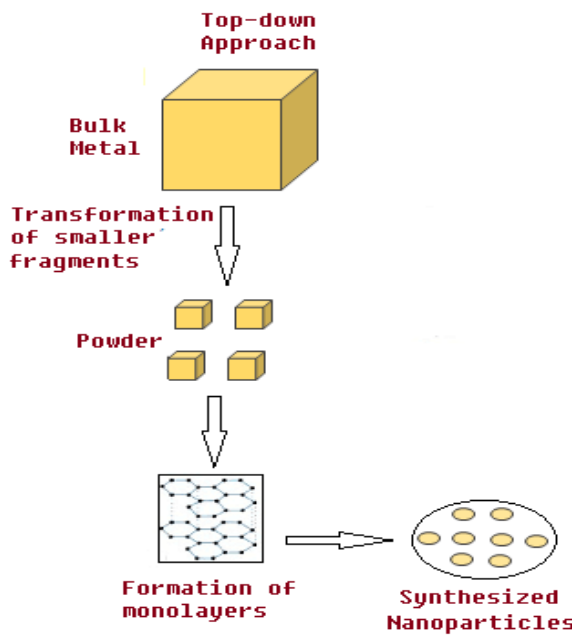


Figure 11: Representation of top down Approach

3.1.3 Bottom-up Approach:

In contrast to top-down approach bottom-up approach starts from miniaturized particles like atoms and molecules that assemble together to form nanomaterials. Self-assembly is the key to bottom-up approach where nanostructures are developed without any external manipulation. Materials formed by this approach are usually found having fewer imperfect surfaces with minimal defects.[36]

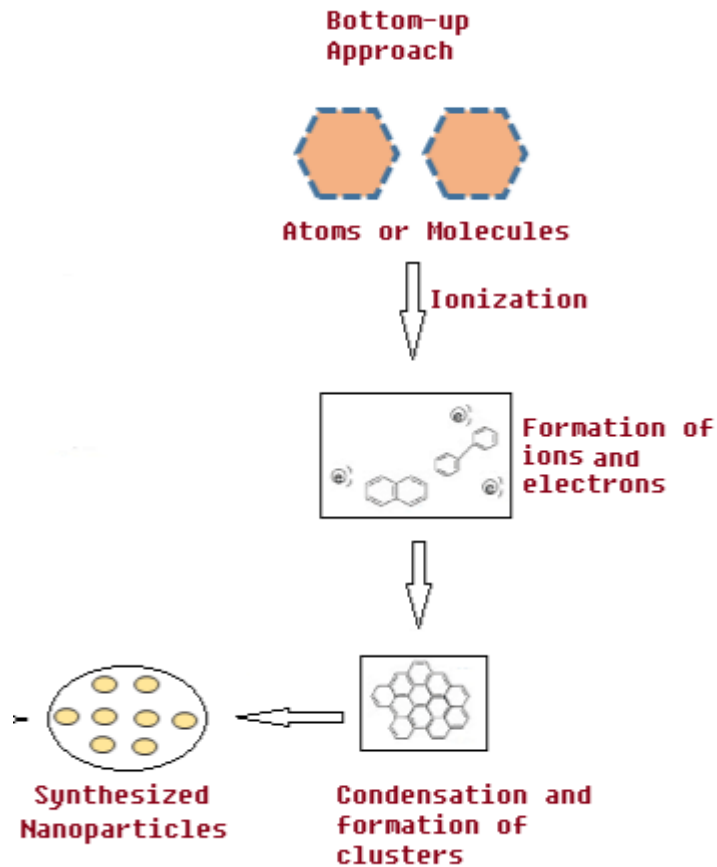


Figure 12: Representation of bottom up Approach

Magnetic properties of the nanomaterials have been investigated to have strong dependence upon the chemical composition, interactions between the particles, particle size, shape of the materials and the preparation method used for the synthesis.

Various methods have been utilized to prepare the nanoparticles those are:

Sol Gel method

Hydrothermal method

Sonochemical processing

Coprecipitation method

Micro emulsion technique

Mechanical milling

Spray pyrolysis

Laser pyrolysis

Depending on the merits and demerits of each method sol gel method have been adopted to synthesize required strontium hexa ferrites.[37]

3.2 Sol Gel Technique:

This technique has been widely used for nanoparticles synthesis since twentieth century. This method is primarily a bottom-up approach. In this technique two or more metal oxides are mixed in certain proportions to form an alloy product. The basic advantage of this method is the homogeneity. In this process a certain number of irreversible reactions usually take place to form the final product. During these irreversible reactions a thick viscous type of solution is formed that is named as gel. Basically, gel is the conversion of nonhomogeneous molecules (sol) into infinite three-dimensional heavy molecule. After the formation of gel drying of gel is performed that leads to rigid solid structure.[38] Nano sized porosity of the final product can be achieved by controlling the drying conditions of the gel. So as nano sized porosity has an advantage of large surface area that is the basic property of nanomaterials. Porous nanomaterials are used to store hydrogen variation in the concentration of the solution constituents or the variation in the pH is usually done to convert sol the gel. The produced gel is found to have the ability of casting and the casting products can be used as membranes or forming. This method is helpful in forming composites and nanocomposite materials. The schematic of sol gel process is as shown below:

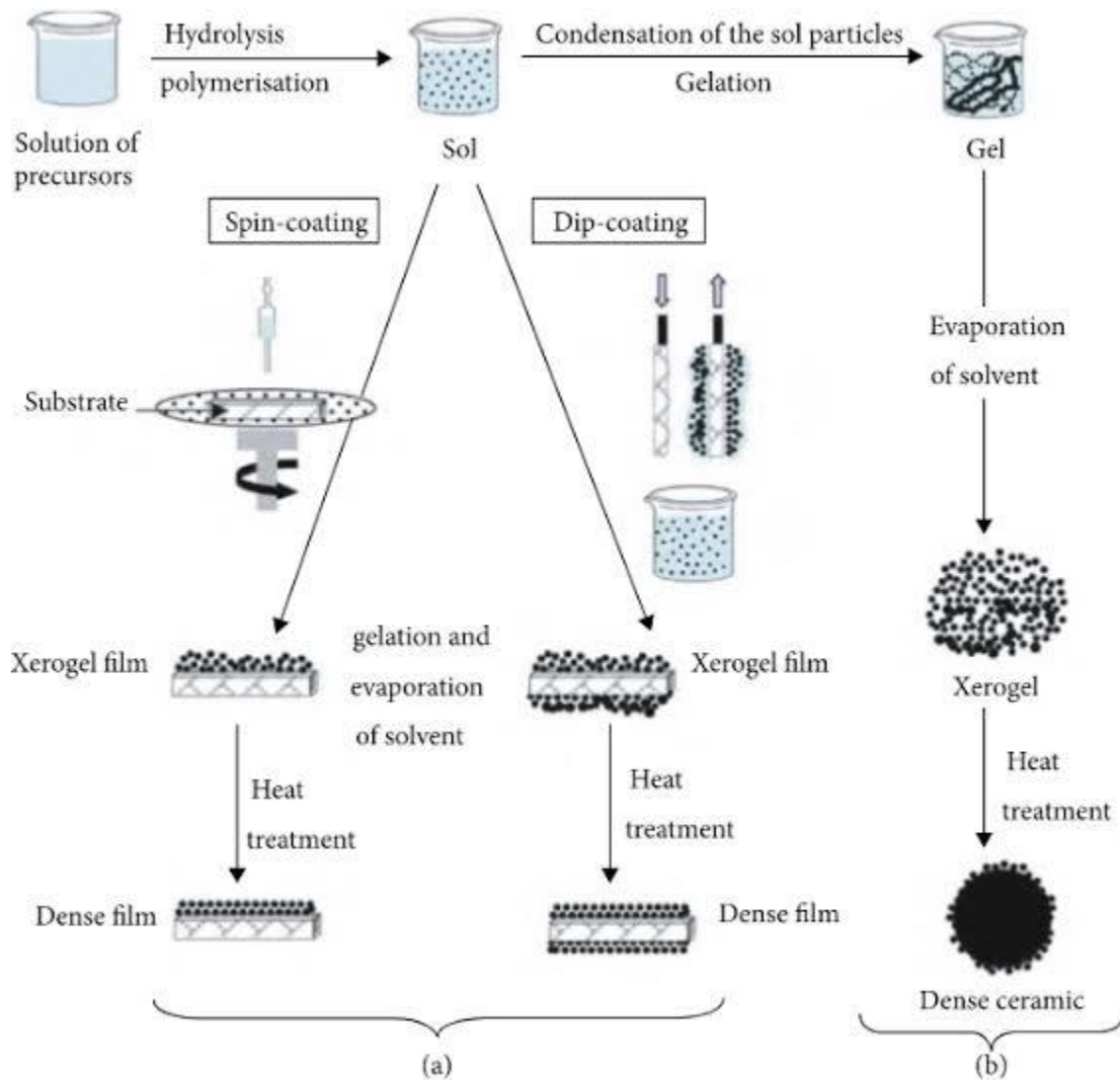


Figure 13: Schematic of Sol gel method for nanoparticles Fabrication

3.2.1 Sol gel process steps:

The basic steps of sol gel technique are as following:

3.2.2 Homogeneous solution formation:

Initially a homogeneous solution by mixing precursors and alcohols is formed. Solvent and precursors are mixed together to produce a homogenous. Solvent can be water , alcohol or

some organic compound of the precursor is metallic salt then organic solvent is not needed because they can dissolve direct in water as well.

Sol Formation:

After the solution of precursors in solvent is prepared then hydrolysis takes place of the solution is homogeneous solution then same organic solvent water is added to perform hydrolysis of solution of metallic salt in water is prepared then there is no need of addition of water. After decomposition of complex compound to simpler one, chemical reaction with water the resulting product is named as a sol.

3.2.3 Gelation:

Sol conversion to gel takes place through condensation reaction where simpler molecules join together to form complex molecule. After the condensation reaction a small molecule like water is released and product is soluble. The product gel then dried to remove the solvent, using any suitable drying method. [39-40]

Solvent separation from gel can be performed either by placing the gel in atmosphere to dry to form xerogel, or by reducing the changes in the network to form aerogel.

3.2.4 Advantages:

Low temperature based process that is helpful in the formation of ceramic nanomaterials b/w low temperature range.

High purity of the product.

Formation of narrow size particles.

High surface coverage.

3.3 Experimental Procedure:

Synthesis of all the samples of pure and doped strontium hexaferrites was performed by following sol gel technique.

3.4 Synthesis of SrFe_{12-2x}(Al, Li, Ni)_xO₁₉

For the synthesis of pure strontium hexa ferrites initially measurement of the required amount of chemical for each solution was done by the use of following formula

$$\text{Molarity} \times \text{Molecular mass} \times 100 / 1000 \dots$$

After calculating required mass of each chemical the solution of strontium nitrates Sr(NO₃)₂ in 100ml deionized water was prepared by constant stirring by using a magnetic stirrer for 15 minutes to attain clear solution in water. Similarly, solution of iron nitrate nonahydrate Fe(NO₃)₃9H₂O in 100 ml deionized water was prepared by constant stirring for 15 minutes by magnetic stirrer. Solution of citric acid in 100ml deionized water was prepared by continuous stirring for 15 minutes by magnetic stirrer to get complete dissolution. All the solutions were added in a large beaker with continuous stirring and after 15 minutes of stirring pH of the solution was neutralized with the drop wise addition of ammonia solution.

Solution remained at continuous stirring and after that done with heating powered on for heating at 90°C. After some time the solution started to be converted to thick gel. After that the thickened gel catches fire, after combustion was completed the heating and stirring set to off. Dark brown coloured powder was obtained which then grinded with the help of mortar and pestle. Final fine powdered samples were calcined at 950°C for 5 hours.

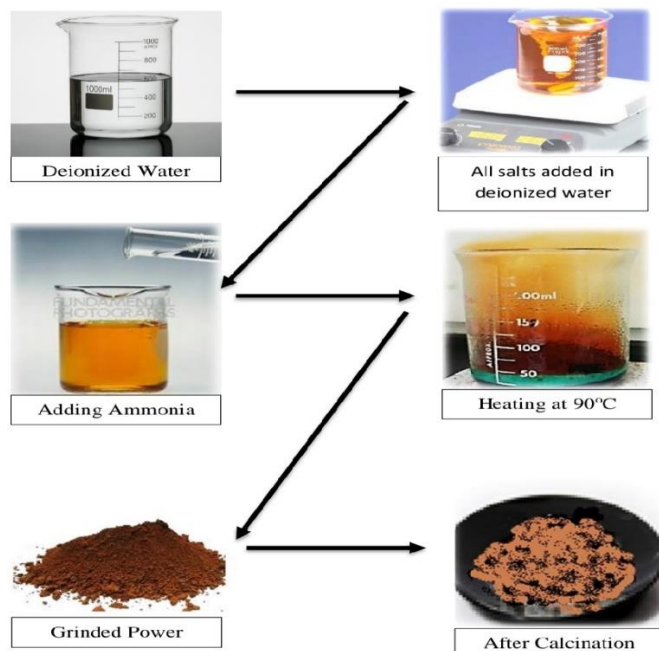


Figure 14: Schematic of synthesis of strontium ferrites by Sol gel method

3.5 Synthesis of Aluminum, lithium and Nickel doped Strontium hexaferrites:

The series of sample of doped strontium hexaferrites was prepared with varying as $x=0.2$, 0.35 and 0.5.

Since the required mass of each chemical was calculated initially by molar mass formula solution of aluminum lithium and nickel nitrate each in 100ml of deionized water was prepared by continuous stirring for 15 min until complete dissolution occurs. Solution strontium nitrate citric acid in 100ml of deionized water was prepared by continuous stirring for 15 minutes. All of the solutions were added in a large beaker, pH was neutralized with drop wise addition of ammonia solution and then heated at 90°C with continuous magnetic stirring until the gelation occurs and solution catches fire. After that heated and stirring were turned Off and dark brown colour powdered samples were obtained. After that samples were grinded and then calcined at 950°C five hours.

Chapter 4

Characterization Techniques

The properties of the synthesized pure and doped strontium hexaferrites were examined through some specific analysis techniques. Structural, chemical, magnetic and dielectric properties and information about lattice parameter and morphology can be obtained by using characterization techniques. This chapter will give a short over view of all techniques used to analyze strontium hexaferrites. Following are the characterization techniques followed:

4.1 X-ray diffraction Technique:

X-rays diffraction is a technique used to determine the nature of material whether it is crystalline or amorphous. It is basically used for the qualitative and quantitative crystalline phase analysis. Furthermore, detailed information like crystal orientation, crystallite size, shape, effect of temperature, impacts of stress and strain at different levels can be obtained through XRD analysis.

In case of ceramic material, the quantity of ratio of iron oxide in a mixture can be obtained through the comparison of intensities of reference peak and an experimental peak. [41]

4.1.1 Working of XRD:

The working principle of X-rays diffraction is based on the constructive interference of monochromatic X-rays after passing through a crystalline sample. These X-rays are produced by a cathode ray tube, which then filtered to generate single beam of monochromatic light. This monochromatic beam of X-rays is then collimated and

subjected towards the sample. The interaction b/w the incident rays and sample can cause the interference to occur whether constructive or destructive. The atoms in the sample are imagined as the family of planes with a spacing. The incident beam is subjected at angle θ . [42]

Constructive interference occurs if the conditions fulfill the Bragg's law i.e.

$$n\lambda = 2d\sin\theta$$

Where the λ is the wavelength, n is the order of reflection, d is the inter-planar spacing and θ is the angle b/w incident beam and crystal lattice planes the diffracted X-rays then detected by the detector and counted.

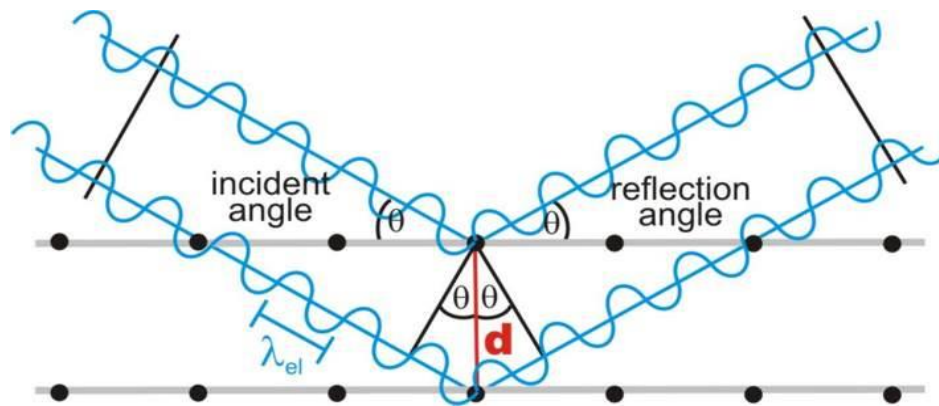


Figure 15: Scattering of Incident X-ray by a plane

In XRD three techniques for the identification of the dimensional crystal structure three methods are usually used those are:

Powder method.

Laue Method

Rotating Crystal Method.

In case of ceramic materials usually ferrites sample is usually prepared in powder form, so powder diffraction method is preferred for sample characterization. [43]

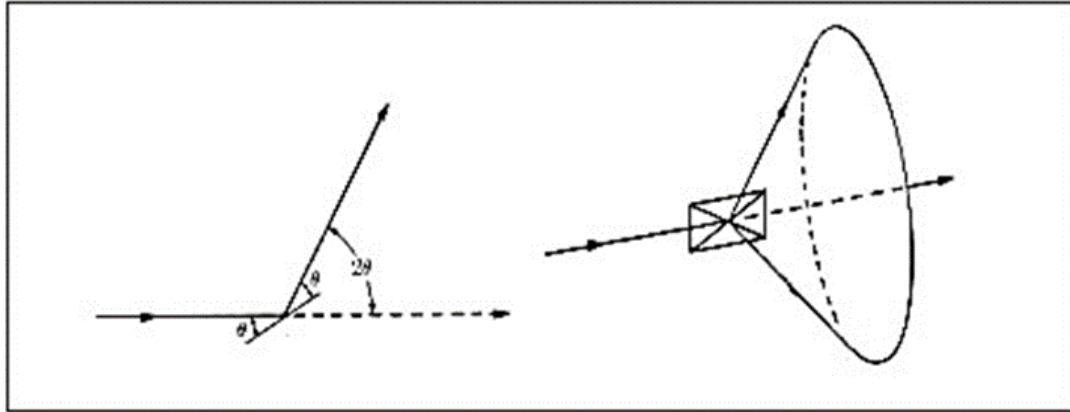


Figure 16: X ray Diffraction

Consider the reflection as shown in figure. The fraction of sample, which is in powder form, is at such an orientation which will enable reflection by being present at correct Bragg angles. When the plane is rotated about the beam which is made incident, the path of motion of reflected beam will be across the surface of cone. In the case of our particles the reflection does not occur across the surface, a large number of crystal particles will have same reflections and some of those reflections will be able to satisfy brags law. The inter planner spacing, d , can be calculated by knowing values of λ and θ .

4.1.2 Powder Diffraction Method:

In powder diffraction method sample is originally grinded to powder form and then placed on a sample holder and monochromatic X-rays are then subjected to fall on the sample. The sample is rotated at an angle θ and the detector is mounted to collect the diffracted rays by the sample, while satisfying the Bragg's law. The inter planner spacing can be calculated by using angle θ and wavelength λ .

4.1.3 Lattice Constant:

In a crystal structure measurement of how closely packed atoms are referred as lattice constant of crystal structure. It is the lattice geometrical configuration as well as the radius of each of the atoms in the crystal structure Lattice constant refers to the spacing b/w the adjacent unit cells in a crystal structure.

Following equation is generally used to calculate the lattice constant

$$\frac{1}{d^2} = \frac{4}{3} \left(\frac{h^2 + hk + k^2}{a^2} \right) + \frac{l^2}{c^2}$$

Where h, k, l are the miller indices, λ is the wavelength of X-rays and θ is the diffraction angle.[44]

4.1.4 Crystallite Size:

Particle size of the material has a huge effect on the structural properties. According to Debye Scherrer equation particle size can be calculated as:

$$t = 0.9 \lambda \beta \cos \theta$$

where λ is incident x-rays wavelength, θ is the diffraction angle and β is the full width half maximum respectively. According to Debye Scherrer equation particle size is inversely proportional to peak width. So peak broadening corresponds to the smaller crystallite size.

4.2 Fourier transform infrared Spectroscopy:

Fourier transform infrared spectroscopy is widely used characterization technique for the identification of functional groups present in materials primarily solid, liquid or gas by utilizing infrared beam of light. A spectrum is obtained b/w wavenumber and % transmittance upon the absorption of infrared radiation by the bonds present in molecules of the material or sample. Infrared radiation contain at low energy and higher wavelength as compared to the UV- visible light and contain high energy and shorter wavelength than microwave radiation.

Material to be analyzed by FTIR should be IR active which means that it should have molecules containing dipole moment. When IR radiation made to fall on the sample it

interacts with the covalent bond b/w the molecules and cause back & fourth movement of the bond and net dipole moment changes and IR radiation gets absorbed.[45].

4.2.1 Basic principle of FTIR:

When the material or sample is exposed to IR radiation the IR active molecules present in the sample absorb the light and then generation vibration modes. So as the absorption of radiation of radiation depends upon the nature of bond present b/w molecules in the sample. The frequency ranges are measured in the form of wavenumbers. FTIR spectrum is obtained as wave number since wavenumbers correlates the frequency and energy. Absorption spectrum represents the different bond vibrations. Different bond vibrations give rise to several modes in the spectrum that counters the identification of different functional groups.

4.2.2 Instrumentation:

The FTIR spectrometer consists of Michelson interferometer, light source sample holder, amplifier detector and compiler, initially light is generated by the light source and enters the interferometers and then passed to the sample and then detected by the detector.

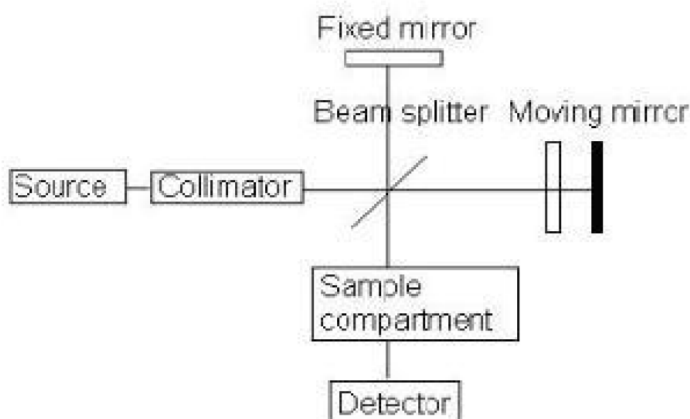


Figure 17: Schematic figure of FTIR

. When the light is generated by the light source and passed to the interferometer it splits it into two beams by beam splitter. Half of the light is transmitted by beam splitter to fixed mirror. Both mirrors reflect back the radiations to the beam splitter, where both reflected beams recombine back to generate single beam and pass it to the sample. After interacting with the sample an interferogram is obtained upon which Fourier transform is applied to obtain the spectrum.[46]

Applications of FTIR:

A gas chromatograph is used to separate the components of a mixture

- The analysis of liquid chromatography fraction can be done using FTIR.
- Tiny samples can be checked with the help of infrared microscope in sample chamber.
- The sample acquiring emitted spectrum of light is obtained FTIR instead of light spectrum through the sample.

4.3 Dielectric:

Dielectric properties measurement depends upon the calculation of dielectric constant, dielectric loss, tangent loss, ac conductivity and elastic modulus. For the measurement of these attributes firstly samples are formed in pellets form and then placed in sample holder of LCR bridge one following formula:

$$\epsilon' = Cd A\epsilon_0$$

here C is the capacitance (farad) d is the thickness of the pellet, ϵ_0 is the permittivity of free space and A is the cross-sectional area of the pellet.

The energy dissipation losses are calculated by the following equation:

$$\epsilon'' = \epsilon' \times D$$

Measurement of dielectric properties takes place using RF impedance analyzer as shown in the following figure:

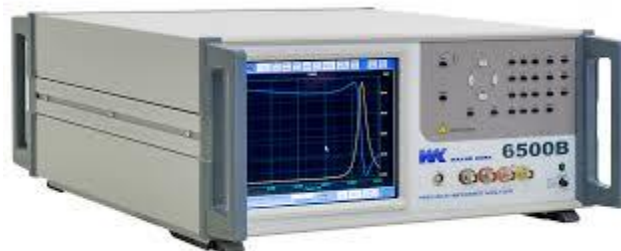


Figure 18: Impedance Analyzer

Dielectric materials upon interaction with applied field get polarized.[47-48] Different types of polarization that take place are as follows:

4.3.1 Dipolar and Orientation Polarization:

When polar dielectric materials are present the absence of the electric field they are randomly oriented and as a result they cancel the effect of each other and their net dipole moment is zero. Consequently, when these materials are placed in electric field they tend to align themselves in the direction of the field.

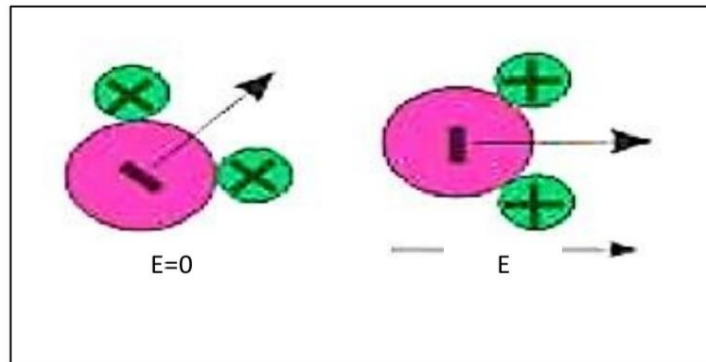


Figure 19: Dipolar Polarization

4.3.2 Ionic Polarization:

In solids having dipoles with ionic bonding ionic polarization takes place but dipoles cancel each other because of symmetry of crystal structure. When electric field is applied positive and negative ions are displaced from their equilibrium position.[49]

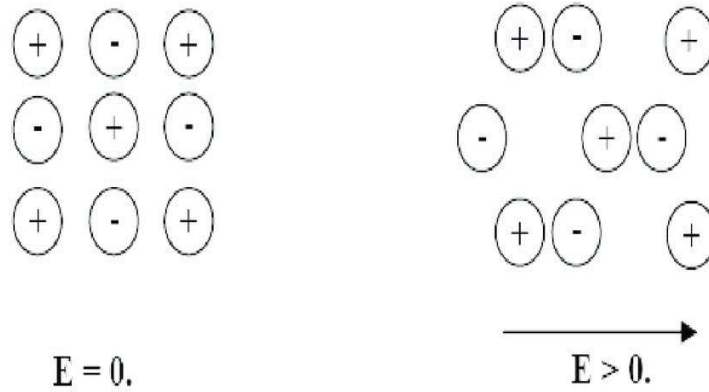


Figure 20: Ionic Polarization

4.3.3 Interface and space charge Polarization:

Space charge polarization take place due to the diffusion of ions along with applied electric filed. It usually occurs due to the accumulation of charges in the interface or at the grain boundaries of the material.

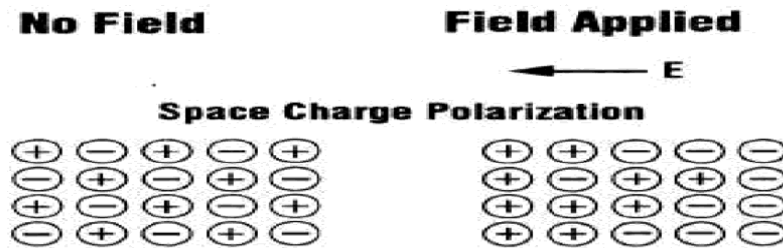


Figure 21: Space Charge Polarization

4.3.4 Electronic and Atomic Polarization:

When the dielectric material is placed within the electric field the electron cloud of atoms is displaced relative to nuclei in atom, which produce an induced dipole moment in the molecule. [50]

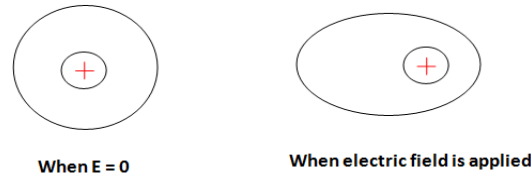


Figure 1

Figure 22: Electronic Polarization

4.4 Vibrating Sample Magnetometry:

Vibrating sample magnetometry is the technique used to analyze the magnetic properties of the materials when placed in the magnetic field. Vibrating sample magnetometer was first designed by the Simon Foner, in 1959. The main goal behind the use of this instrument is to find the magnetic properties of all the magnetic materials like paramagnetic, diamagnetic, ferromagnetic, ferrimagnetic and anti-ferromagnetic at varying temperatures.

4.4.1 Working Principle:

Vibrating sample magnetometer works on the basic principle of Faraday's law of electromagnetic induction. According to magnetic law of induction magnetic moment of the material is obtained when it is placed in uniform magnetic field and starts vibrating perpendicular to the field. The coils are stationary with respect to the vibrating sample. Any change in applied field generates voltage in stationary coils.

4.4.2 Instrumentation:

A rod is used as sample holder to hold sample between coils. The holder is attached to a vibration exciter that vibrates the sample at constant frequency. Rod is rotated to expose different orientations of the sample to constant magnetic field. Constant magnetic field is provided by water cooled electromagnet. Sample vibrations at constant frequency generate

alternating current in the sensor coils that generate signal and pass it to amplifier for amplification. Collection of data is done through computer.[51]

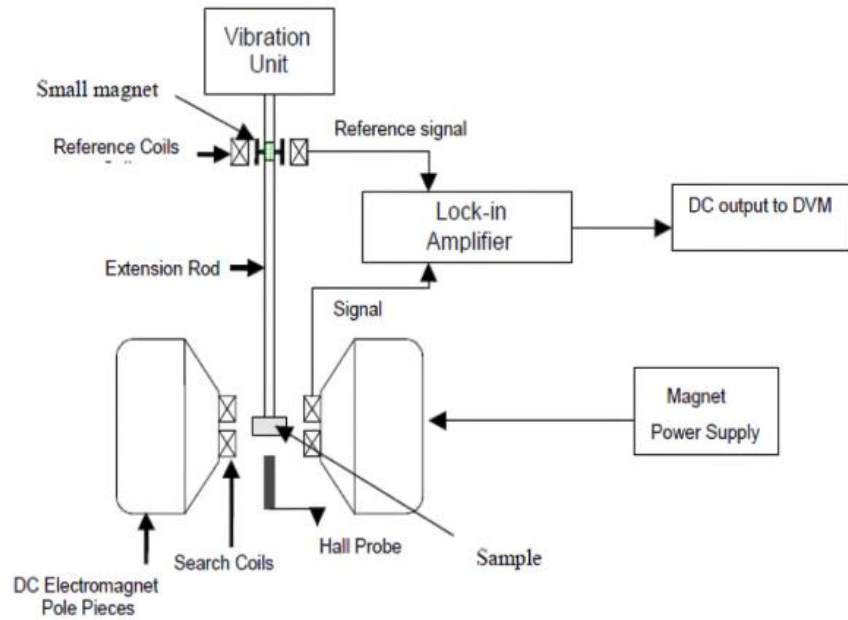


Figure 23: Schematic of VSM

Chapter 5

Results and Discussion:

5.1 XRD Analysis:

X-ray diffraction technique gives useful information about phase and structure of the material. To perform structural analysis of pure and doped strontium ferrites all of the samples were grinded to fine powder and then annealed at 950°C before subjecting to XRD. The XRD peaks for pure strontium hexaferrites are shown in below figure:

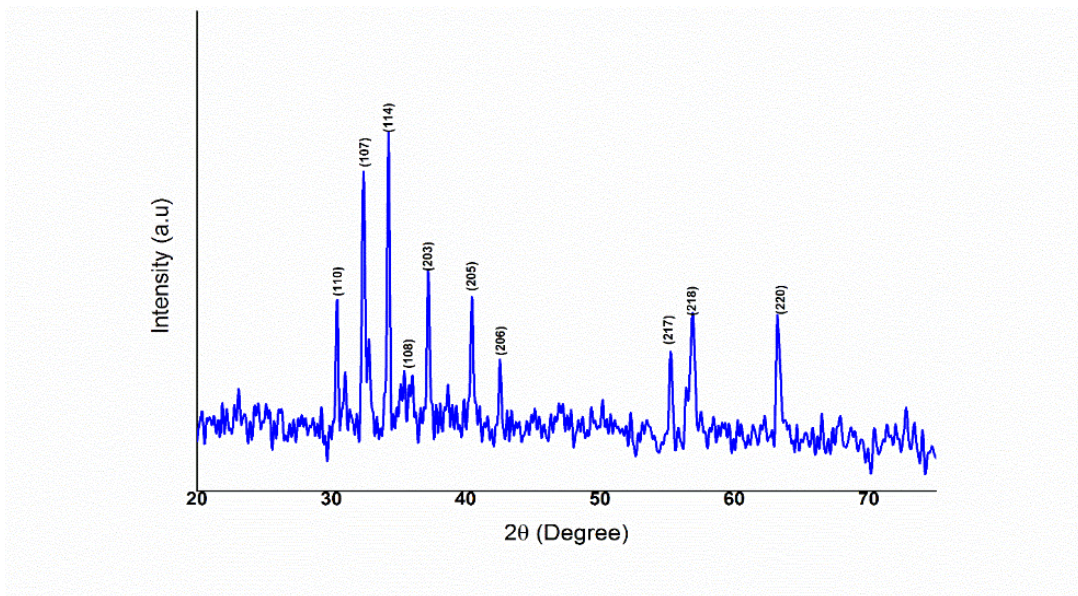


Figure 24: XRD pattern of pure strontium hexaferrites

It can be observed that the diffraction peaks appear at planes (110), (107), (114),(108), (203), (205), (206), (217), (218), (220) present at angles of $2\theta=30.378, 32.304, 34.196, 35.715, 37.137, 40.397, 42.528, 55.187, 57.519$ and 63.252 .The peak positions at specific angle match with JCDPS card no. 00-024-1207.No any other secondary peak appeared that confirmed that there is no extra hematite phase. Through analysis formation of single-phase hexagonal strontium ferrites has been confirmed.

5.1.1 Strontium Hexaferrite doped with Al, Li, Ni [$\text{SrFe}_{12-2x}(\text{Al, Li, Ni})\text{O}_{19}$]:

Strontium hexaferrites was doped with aluminum, lithium and nickel with various concentrations of the dopants. All the doped strontium hexaferrites samples were then annealed at 950°C before subjected to XRD.After analyzing the data by matching with JCDPS card no 00-024-1207.Following figure shows the XRD pattern of doped strontium hexaferrites.

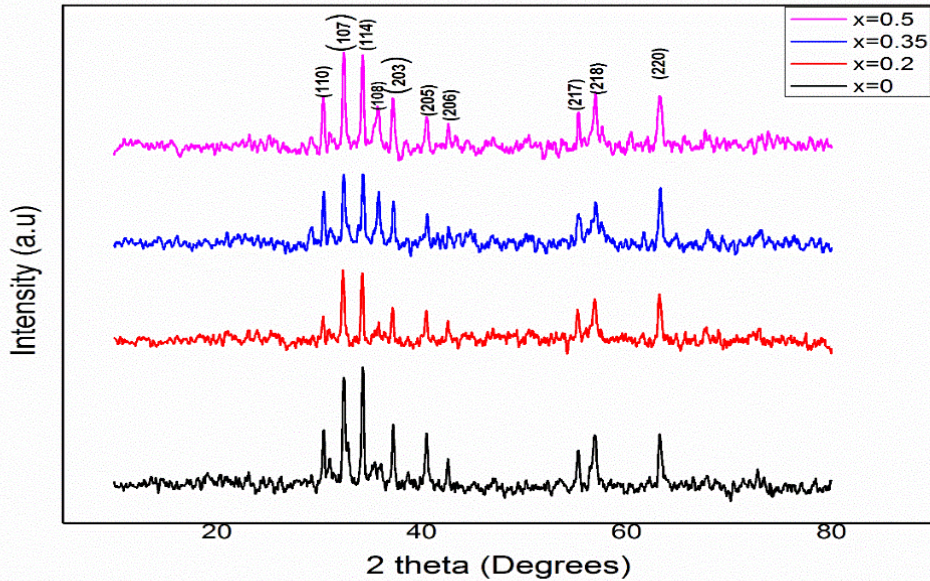


Figure 25 : XRD pattern of doped strontium hexaferrites

. It can be observed that there appears no separate peak just like pure samples confirming the formation of single-phase hexagonal crystal structure. The peaks of both pure and doped strontium ferrites are almost in differentiable because no secondary extra hematite phase formed. The ionic radii of the doped element was comparable to that of iron suggesting that cations are accumulated at tetrahedral sites.

Lattice constant and crystallite size was calculated by using the following equation:

$$\frac{1}{d^2} = \frac{4}{3} \left(\frac{h^2+hk+k^2}{a^2} \right) + \frac{l^2}{c^2}$$

Here h, k, l are miller indices whereas a and c are lattice parameters.

Table 1: Lattice Parameters and crystallite size of pure and doped strontium hexaferrites

Sr No.	Prepared Sample	Lattice Parameter a=b (nm)	Lattice Parameter c (nm)	Crystallite Size (nm)
1	SrFe _{12-2x} (Al, Li, Ni) _x O ₁₉ for x=0	5.87	23.07	35.43
2	SrFe _{12-2x} (Al, Li, Ni) _x O ₁₉ for x=0.2	5.88	23.08	33.14
3	SrFe _{12-2x} (Al, Li, Ni) _x O ₁₉ for x=0.35	5.89	23.08	30.00
4	SrFe _{12-2x} (Al, Li, Ni) _x O ₁₉ for x=0.5	5.89	23.09	27.61

By detailed XRD it has been evaluated that with variation in dopant's concentration in strontium hexaferrites there comes slight change in lattice parameters “a” and “c” and the crystallites size increases. All these attributes are correlated to the minimal change between ionic radii of substituted cations and iron.

5.2 Ftir:

Fourier transform infrared spectroscopy is a useful technique that illustrates the nature of chemical bonds present in the material. Pure and doped strontium hexaferrites powdered samples were mixed with potassium bromide and then by hydraulic press converted into pellets. The frequency range was 2500cm^{-1} to 350cm^{-1} . FTIR gives useful information about cations distribution at tetrahedral and octahedral sites. The plot of wave number versus percentage transmittance for pure and doped strontium ferrites is shown in following figure:

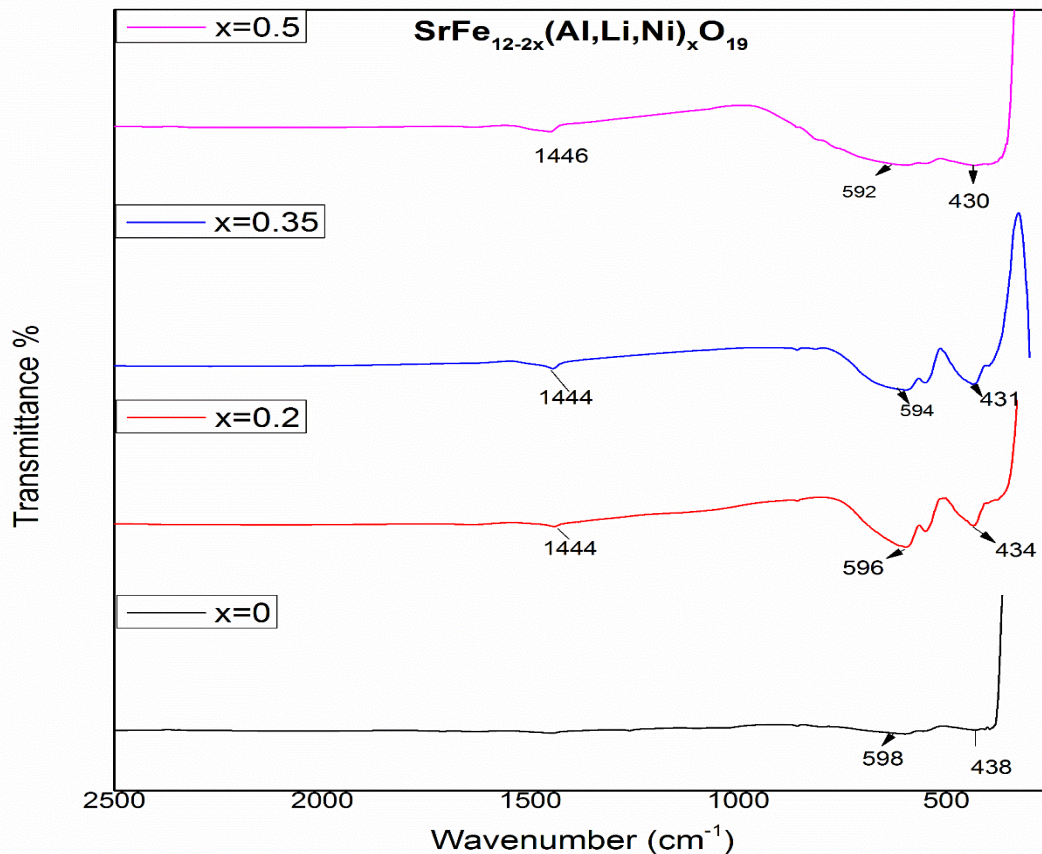


Figure 26: FTIR Spectrum

The infrared spectrum was well explained by the Waldron according to him each spectrum contains ν_1 and ν_2 two absorption bands that correspond to stretching vibrations of metal and oxygen bonds present in tetrahedral and octahedral sites. The band position differs for tetrahedral and octahedral site due to difference in bond length of Fe-O. The observed spectrum for each sample of pure and doped strontium ferrites confirmed the formation of hexagonal strontium hexaferrites. The vibrational frequency of the tetrahedral site is higher as compared to the octahedral site corresponding to the shorter bond length of tetrahedral site. It can be observed from the spectrum that with the increase in dopant's concentration from $x=0$ to $x=0.5$ the tetrahedral vibrational frequency shifted toward a lower frequency range. This can be related to the replacement of the Fe^{+3} ions by the substituted cations.

Since the bond length increases at the tetrahedral site the vibrational frequency shifted to lower range.

Dielectric Analysis:

Dielectric properties of pure and doped synthesized samples were measured by using Wayne Kerr precision analyzer. Dielectric constant, dielectric loss, tangent loss and ac conductivity have been studied by using the instrument. Characterization was performed by preparing the samples in the form of pellets by using 10mm die. The weight of the powder was kept up to 0.9g and prepared pellets were sintered. Since the dielectric materials are usually considered as the insulators but their attribute of having capability to get polarized under the applied electric field makes them suitable for the various applications like shielding.

5.3 Dielectric Constant:

The permittivity of the substance also known as dielectric constant represents the energy storage capability of a material when it is subjected to an applied electric field. Dielectric measurement includes a real and imaginary part. When a magnetic field is applied to a material it undergoes polarization that is represented by the real part. Various models have been used to briefly describe the dielectric properties of the materials. One of such model was proposed by Maxwell- Wagner who explained the mechanism of space charge polarization in dielectric materials. According to this model a dielectric material has grain and grain boundaries. The boundary behaves as high resisting layer whereas grain acts as conductor due to which space charge polarization occurs. The dielectric polarization mechanism in ferrites resembles to their conduction mechanism i.e. hopping between electrons of same element occurs. This assumption can be correlated with large dielectric constant at low frequency since at low frequency hopping between electrons follows the applied electric field and material gets polarized as a result dielectric constant increase. Contrary to this at high frequency the hopping between electrons could not follow the applied electric field and as a result dielectric constant decrease. Pure and doped strontium hexa ferrites samples in the the form of pellets were subjected to the Kerr precision analyzer sequentially according to dopant's concentration. The frequency range was kept from

1MHz to 1GHz to study the dielectric constant. The graph of dielectric constant shown below for pure and doped strontium hexa ferrites shows that the dielectric constant increases at low frequency since when the external field is applied the electrons start to move towards the grain boundaries and get accumulated there. Accumulation of electrons at the grain boundaries results in polarization of the material and as a result dielectric constant attains higher values at low frequency. It can be observed from the below dielectric plots that with the increasing frequency the dielectric constant started to decrease and eventually became constant. This decrement in dielectric constant can be well explained through Wanger model that is at higher frequencies hopping between the electrons cannot follow the applied electric field that slows down the movement of electrons and as a result dielectric constant decrease.

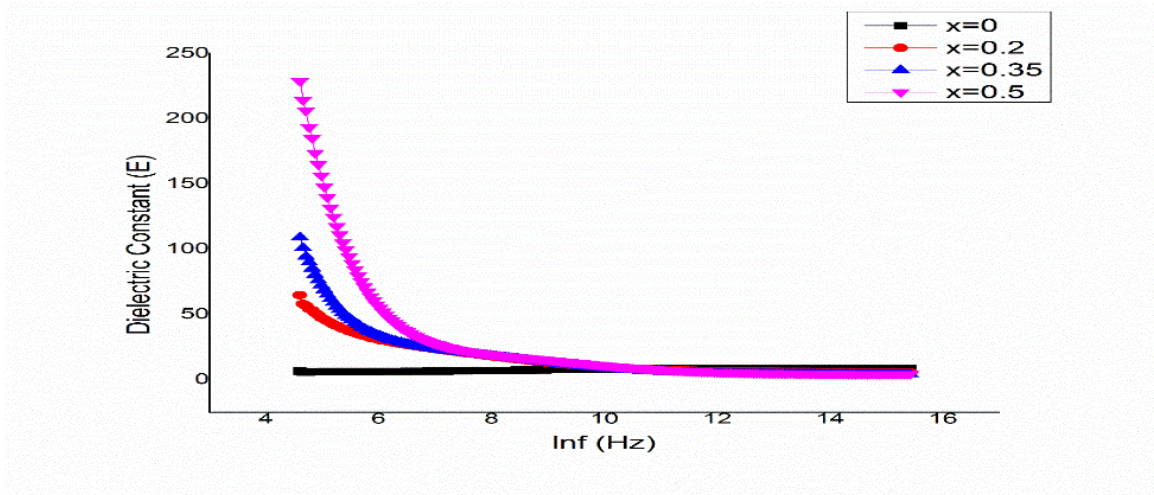


Figure 27: Dielectric Constant Variation with frequency

It can be observed that the dielectric constant increased with increasing dopant's concentration as the doped cations are accumulated at the tetrahedral sites. They tend to move Fe^{+3} ions towards the octahedral sites and hence hopping between Fe^{+2} and Fe^{+3} takes place resulting in polarization and hence dielectric constant increased.

Table 2: Dielectric constant of pure and doped strontium hexaferrites

Sample	Dielectric constant
SrFe_{12-2x} (Al, Li, Ni)_xO₁₉ for x=0	6.310
SrFe_{12-2x} (Al, Li, Ni)_xO₁₉ for x=0.2	57.79
SrFe_{12-2x} (Al, Li, Ni)_xO₁₉ for x=0.35	108.88
SrFe_{12-2x} (Al, Li, Ni)_xO₁₉ for x=0.5	228.60

5.4 Dielectric Loss:

The imaginary part of the dielectric constant is termed as the dielectric loss or loss factor is the amount of the energy dissipated. Pure and doped strontium hexaferrites were examined in respect of dielectric loss changes with frequency. The figure below represents the change in dielectric loss with frequency.

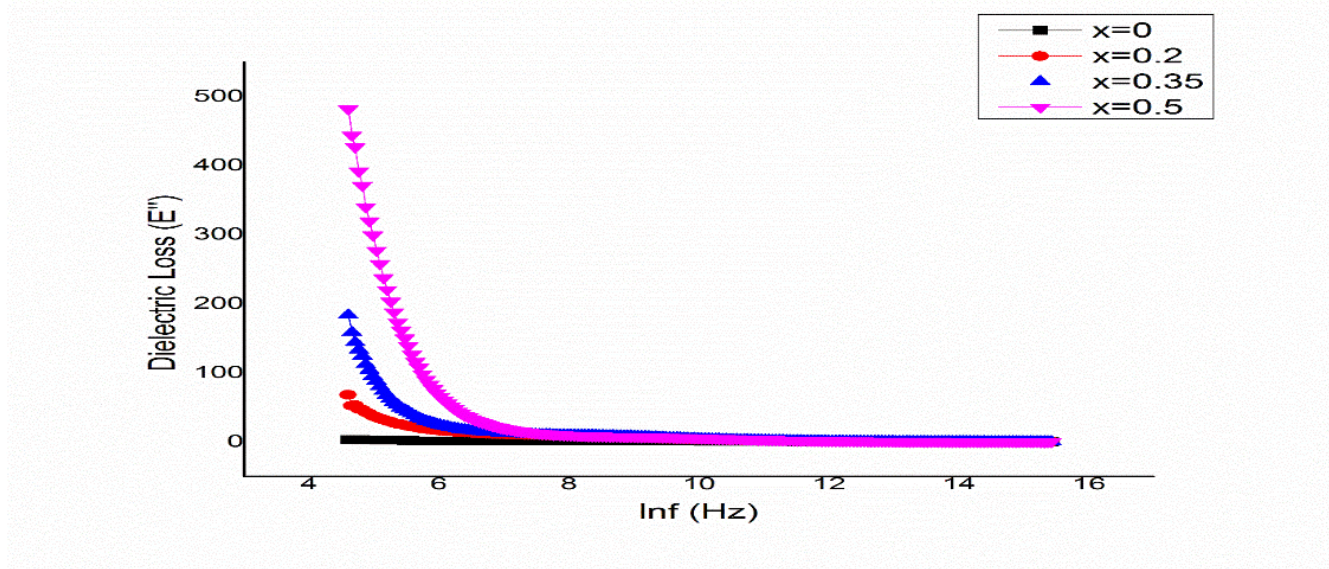


Figure 28: Dielectric loss variation with Frequency

The change in dielectric loss with respect to frequency can be observed as almost same as dielectric constant. Initially at lower frequency the dielectric loss is higher and with the increase of frequency the dielectric loss is decreases and above a certain frequency it becomes constant. There seems an inverse relation between frequency of applied field and dielectric loss. This attribute of variation of dielectric loss with frequency is well explained by Koop's theory. According to Koop's theory at lower frequency of applied field the resistance offered by grain boundaries is higher corresponding to the high energy requirement for the electrons for the hopping between the charge carriers and hence more energy is required for polarization to occur and there comes high dielectric loss or energy loss. At higher frequency of the applied field the resistance offered by the grain boundaries is lower corresponding to the low energy requirement for the electrons for the hopping between the charge carriers and less energy is required for the polarization to occur and energy loss is low and eventually becomes constant. The decreasing trend of dielectric loss with increasing frequency can also be related to the factor that the electrons has less ability to align themselves along the quickly alternating applied field due to less jumping of electrons between the hoping places as the frequency of alternating filed is much high and

the frequency of electrons is less as compared to that. Since the high frequency sections correspond to the highly dominant grains having provided low conductivity.

It can be observed that the dielectric loss increases with the increase in dopant's concentration it can be related to replacement of the Fe^{+3} ions by the doped cations and hence the less hopping corresponding to the less energy consumption.

Table 3: Dielectric loss of pure and doped strontium hexaferrites

Sample	Dielectric loss
SrFe_{12-2x} (Al, Li, Ni)_xO₁₉ for x=0	2.9477
SrFe_{12-2x} (Al, Li, Ni)_xO₁₉ for x=0.2	68.018
SrFe_{12-2x} (Al, Li, Ni)_xO₁₉ for x=0.35	183.69
SrFe_{12-2x} (Al, Li, Ni)_xO₁₉ for x=0.5	482.11

5.5 Tangent Loss:

The ratio of complex or imaginary part of permittivity to real part is known as tangent loss. The major part of whole core loss in ferrites is dielectric tangent loss. It quantifies the relative energy loss due to the applied alternating electric field. There are basically two types of mechanisms contributing to the tangent loss factor of the dielectric properties exhibited by the ferrites, one is electron hopping and the other is polarization dipoles. Electron hopping mechanism dominates the tangent loss factor at the lower frequencies.

The figure below shows the relationship between dielectric tangent loss and alternating frequency of applied field.

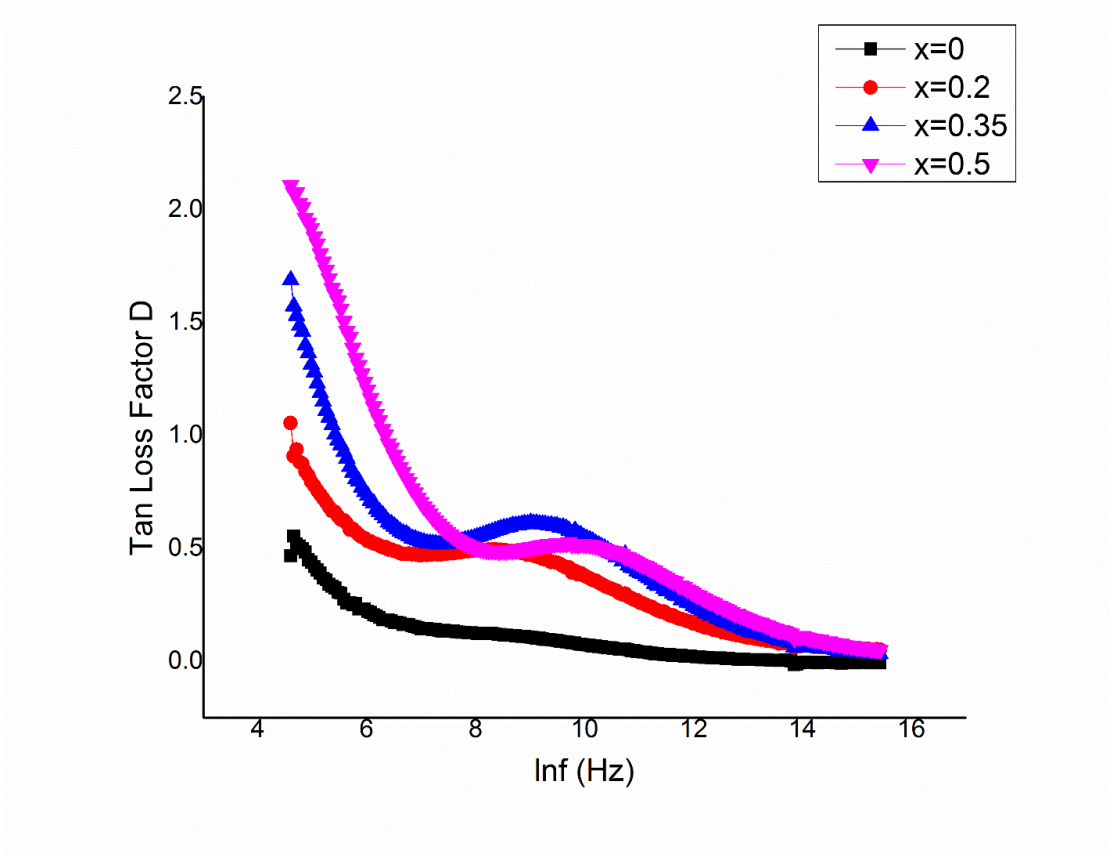


Figure 29 : Tangent loss variation with Frequency

At lower frequencies the dielectric tangent loss has higher values this can be attributed to high energy requirement for the hopping of electrons as at lower frequencies high retardation is offered by the grain boundaries and the grains. As a result, there will come a delay in polarization orientation dipoles response to the alternating applied field which explains high tangent loss at lower frequency. Furthermore, the presence of imperfections

and defects also contribute to the energy loss. On the other hand, at higher frequencies hopping of electrons reduces with low energy consumption corresponding to the decrease in tangent loss factor. This inverse relationship between tangent loss and frequency can be quantified as since at lower frequencies the resistivity of grain boundaries is higher that hinders the hopping of electrons so as polarization and high energy losses are observed and at higher frequencies of applied field the resistivity of grain boundaries is less resulting in low energy losses.

Table 4: Tangent loss of pure and doped strontium hexaferrites

Sample	Tangent loss
SrFe_{12-2x} (Al, Li, Ni)_xO₁₉ for x=0	0.55297
SrFe_{12-2x} (Al, Li, Ni)_xO₁₉ for x=0.2	1.0542
SrFe_{12-2x} (Al, Li, Ni)_xO₁₉ for x=0.35	1.6870
SrFe_{12-2x} (Al, Li, Ni)_xO₁₉ for x=0.5	2.1089

The tangent loss plot clearly depicts that the tangent loss is increasing with the increasing dopant concentration. Tangent loss has low values for the pure strontium hexaferrites and attained higher values with increasing dopant's concentration. This increase of tangent with increasing dopant concentration can be related to the factor of increase in number of charge carriers in doped samples that require high energy for polarization to occur so as contributing to the high tangent loss factor.

AC Conductivity:

The conductive or resistive properties of a material are measured by its conductivity. The conductivity of a material is the measurement of how conductive or resistive it is. The mechanism of conductivity in ferrites is caused by electrons jumping between ions of the same element with different valence states. We computed the conductivity of all the samples in our study by using the following formula:

$$\sigma_{ac} = 2\pi f \epsilon_0 \epsilon''$$

The frequency was represented by f , the permittivity of open space was represented by ϵ_0 and the dielectric loss was represented by d . Figure below depicts the trend of ac conductivity with respect to the frequency. Interfacial polarization of the Maxwell-Wagner type can be used to explain the observed behavior. According to which at lower frequency the grain boundaries become more dominant and offer high resistance to the hopping of electrons and as result the ac conductivity has smaller values at low frequency of the applied field. Since ac conductivity is mainly due to the hopping of electrons so at low frequency this phenomenon occurs very difficultly. Due to the significant impediment imposed by grain boundaries, conductivity is low at lower frequencies. The ac conductivity plot verifies that at higher frequency range the ac conductivity increases that corresponds to the fact that at high frequency less hindrance is offered by the grain boundaries to the hopping of electrons that becomes a source of feasible occurrence of the hopping of electron resulting into the high ac conductivity values.

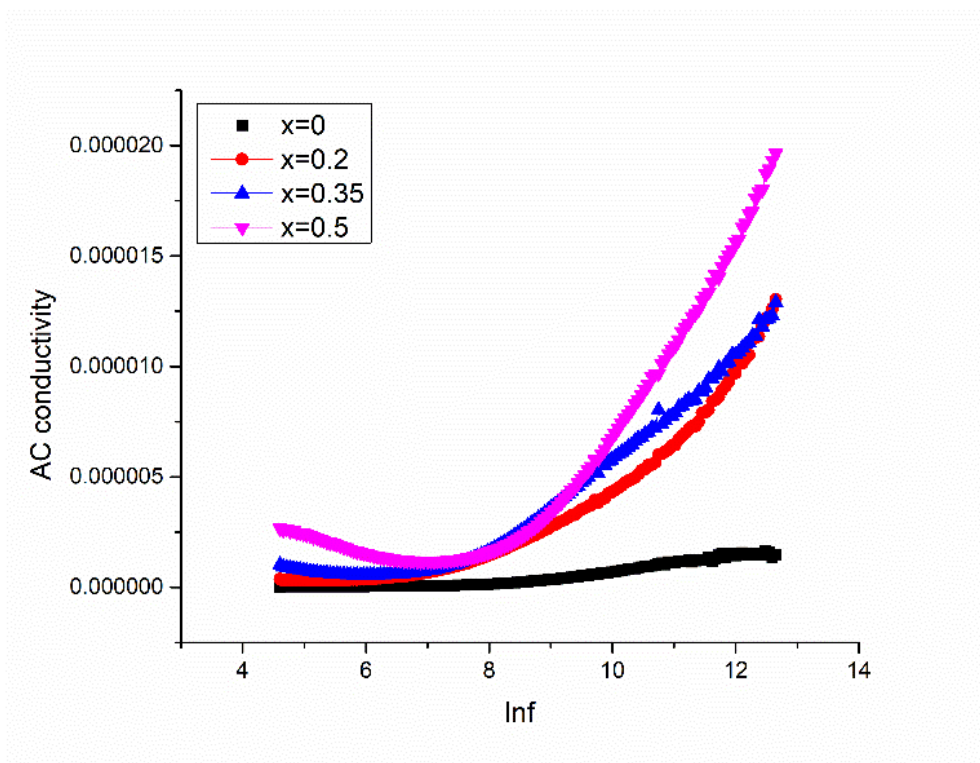


Figure 28: Variation of AC Conductivity with Frequency

It can be observed through ac conductivity plot analysis that the ac conductivity increases with the increase in dopant concentration from $x=0$ to $x=0.5$ due to the reduction in availability of charge carriers.

Table 5: Ac conductivity plot for pure and doped strontium hexaferrites

Sample	AC conductivity
$\text{SrFe}_{12-2x}(\text{Al, Li, Ni})_x\text{O}_{19}$ for $x=0$	1.063
$\text{SrFe}_{12-2x}(\text{Al, Li, Ni})_x\text{O}_{19}$ for $x=0.2$	1.638
$\text{SrFe}_{12-2x}(\text{Al, Li, Ni})_x\text{O}_{19}$ for $x=0.35$	2.020

SrFe_{12-2x} (Al, Li, Ni) _xO₁₉ for x=0.5	2.6794
---	--------

5.6 VSM:

Vibrating sample magnetometer is used for the determination of magnetic properties such as saturation magnetization (**Ms**), coercivity (**Hc**) and remanence (**Mr**). Pure and doped strontium hexaferrites **SrFe_{12-2x} (Al, Li, Ni) _xO₁₉** powder samples were analyzed magnetically through vibrating sample magnetometer. The magnetic hysteresis for pure and doped materials is obtained by plotting VSM data. The M-H loops clearly confirms the magnetic behavior of pure and doped strontium ferrites as having high saturation and coercivity values. Strontium hexaferrites with chemical composition **SrFe_{12-2x} (Al, Li, Ni) _xO₁₉** doped with aluminum lithium and nickel at various concentrations with x varying from zero to 0.5.

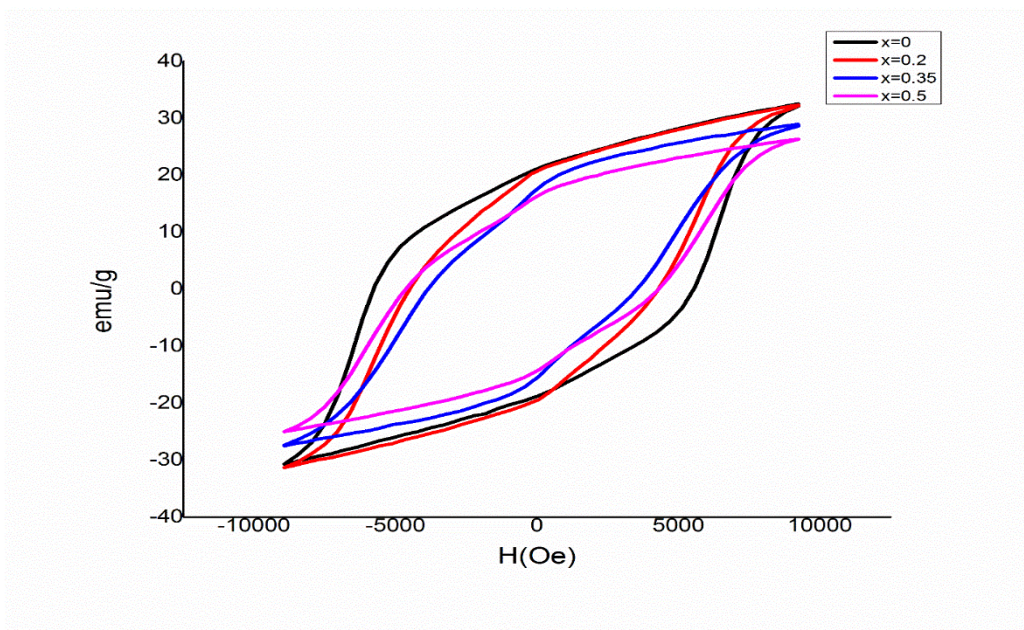


Figure 30: Hysteresis loop for pure and doped strontium ferrites

The M-H loop combine for all the samples represents that the saturation magnetization decreases from $x=0$ to $x=0.5$. This can be because of distribution of cations at various interstitial sites. In M type hexagonal ferrites there are five interstitial sites such as one tetrahedral site(4f1), three octahedral sites (2a ,12k, 4f2) and one trigonal pyramidal site (2b). The sites (4f1 and 4f2) are antiparallel to each other whereas the sites (2a ,12k and 4f2) are parallel to each other.

In ferrites the magnetic ions with spin up and spin down at the interstitial sites give rise to magnetism. If the substitution of cations takes place at interstitial sites with spin up the saturation magnetization decreases and if the substitution of cations takes place at interstitial sites with spin down the saturation magnetization increases. This can be related as the substitution of Al^{+3} , Ni^{+2} and Li^{+1} ions takes place at the 2a and 12k sites with spin up which as a result decreases the net magnetic moment and consequently saturation magnetization decreases. Other parameters like coercivity and remanence also decreased with increasing dopant's concentration from $x=0$ to $x=0.5$. Initially the remanence magnetization for pure sample was 19.98 emu/g and then started gradually decreasing and reached up to 25.62 emu/g. Similarly, coercivity for pure sample was 565.7 at $x=0$ and then decreased up to 307.8 at $x=0.5$. The decrement in these properties is proposing that the material is moving towards being softer.

Table 6: Values of saturation magnetization, remanence and coercivity for pure and doped strontium ferrites

Sr No.	Sample	Ms (emu/g)	Mr (emu/g)	Hc (kAm⁻¹)
1	SrFe _{12-2x} (Al, Li, Ni) _x O ₁₉ for x=0	31.38	19.98	565.7
2	SrFe _{12-2x} (Al, Li, Ni) _x O ₁₉ for x=0.2	32.6	18.08	457.2
3	SrFe _{12-2x} (Al, Li, Ni) _x O ₁₉ for x=0.35	27.98	16.50	367.9
4	SrFe _{12-2x} (Al, Li, Ni) _x O ₁₉ for x=0.5	25.68	15.34	308.4

Conclusion:

We have performed successful synthesis of pure and doped strontium hexaferrites by simple and cost-effective sol gel method. XRD analysis confirmed the formation of single-phase hexagonal strontium hexaferrites. There appeared no such peak that can declare the presence of any impurity in the synthesized samples both for the pure and doped materials. Lattice parameters and crystallite size were calculated by analyzing XRD peaks and comparing the data with JCDPS card no 00-024-1207. Crystallite size has been calculated by using Debye Scherrer equation which came out in the range of 27nm to 35nm. FTIR analysis revealed that the tetrahedral vibrational frequency shifted towards the lower frequency with the increase in dopant's concentration for $x=0$ to $x=0.5$ since the Fe^{+3} ions are replaced by the dopant cations. The dielectric properties of all the samples have been studied through LCR meter. Dielectric constant showed decreasing trend with the increasing frequency due to the mechanism of polarization occurrence at lower frequency. Materials get polarized due to the hopping between electrons that follows the applied field at lower frequency as a result dielectric constant increases. Dielectric loss also appeared to have larger values at lower frequency range due to high hindrance offered by the grain boundaries and hence high energy is required for the polarization to occur. At higher frequencies less hindrance is offered by the grain boundaries that become a cause behind decreasing dielectric losses. Tangent loss showed the same behavior as dielectric constant and dielectric loss due to high hopping of electrons at low frequency. High hindrance offered by grain boundaries at low frequency gave rise to low conductivity values. By VSM analysis saturation magnetization and coercivity found to be decreased with increasing dopant concentration due to accumulation of cations at interstitial sites with upward spin. The materials can be better for use in electrical and magnetic applications.

Future Work

Electrical and magnetic properties of $\text{SrFe}_{12-2x}(\text{Al, Li, Ni})_x\text{O}_{19}$ can be studied by varying the concentration of doped elements or by doping with some other metals.

Composites with different polymers can be made to study electrical, mechanical, and optical properties.

Microwave properties of the samples can be studied for microwave application.

References

- [1] Gandotra, K., & Randhawa, B. S. (2008). Mössbauer studies of nanosized ferrites prepared by the combustion of metal nitrates–oxalyl dihydrazide solutions. *Hyperfine Interactions*, 185(1), 139-143.
- [2] Kumari, V., Dey, K., Giri, S., & Bhaumik, A. (2016). Magnetic memory effect in self-assembled nickel ferrite nanoparticles having mesoscopic void spaces. *RSC advances*, 6(51), 45701-45707.
- [3] Bharamagoudar, R. C., Patil, A. S., Vijay, S. N. M., Laxmi, M. K., & Kankanawadi, B. (2018). Magnetic and antibacterial studies of nanoferrites prepared by self propagating high-temperature synthesis route. *Acta Chemica IASI*, 26(2), 249-262.
- [4] Bouet, L., Tailhades, P., Pasquet, I., Bonningue, C., Le Brun, S., & Rousset, A. (1999). Cation-deficient spinel ferrites: application for high-density write-once optical recording. *Japanese journal of applied physics*, 38(3S), 1826.
- [5] Huang, X., Zhang, J., Lai, M., & Sang, T. (2015). Preparation and microwave absorption mechanisms of the NiZn ferrite nanofibers. *Journal of Alloys and Compounds*, 627, 367-373.
- [6] Liu, H., Sun, K., Yang, Y., Yu, Z., Wu, C., Jiang, X., & Lan, Z. (2015). Study on the contribution of magnetization mechanisms in NiZn ferrites. *IEEE Transactions on Magnetics*, 51(11), 1-4.
- [7] HILGENDORFF, M., & GIERSIG, M. (2012). Properties and Applications. *Low-Dimensional Systems: Theory, Preparation, and Some Applications*, 91, 151.
- [8] Coutinho, D. M. (2019). Synthesis, Characterization and Solid State Properties of Doped Ni and Co Ferrites and their Applications (Doctoral dissertation, Goa University).
- [9] Ishino, K., & Narumiya, Y. (1987). Development of magnetic ferrites: control and application of losses. *AM. CERAM. SOC. BULL. Am. Ceram. Soc. Bull.*, 66(10), 1469.

- [10] Mangai, K. A., Sureshkumar, P., Priya, M., & Rathnakumari, M. (2014). Structural and magnetic properties of strontium hexa-ferrites for permanent magnets. *International Journal of Scientific & Engineering Research*, 5(3), 65-69.
- [11] Atif, M., Nadeem, M., Grössinger, R., & Turtelli, R. S. (2011). Studies on the magnetic, magnetostrictive and electrical properties of sol-gel synthesized Zn doped nickel ferrite. *Journal of Alloys and Compounds*, 509(18), 5720-5724.
- [12] Kalyane, S., & Pathan, A. N. (2021). *COMBUSTION SYNTHESIZED PHYSICAL PROPERTIES OF SOME NANOCRYSTALLINE SUBSTITUTED SPINEL FERRITES SYSTEMS*. Horizon Books (A Division of Ignited Minds Edutech P Ltd).
- [13] Anis-ur-Rehman, M., Ali Malik, M., Khan, K., & Maqsood, A. (2011). Structural, electrical and magnetic properties of nanocrystalline Mg-Co ferrites prepared by Co-precipitation. In *Journal of Nano Research* (Vol. 14, pp. 1-9). Trans Tech Publications Ltd.
- [14] Hessian, M. M., Rashad, M. M., & El-Barawy, K. (2008). Controlling the composition and magnetic properties of strontium hexaferrite synthesized by co-precipitation method. *Journal of magnetism and magnetic materials*, 320(3-4), 336-343.
- [15] Iqbal, M. J., Ashiq, M. N., & Gul, I. H. (2010). Physical, electrical and dielectric properties of Ca-substituted strontium hexaferrite (SrFe₁₂O₁₉) nanoparticles synthesized by co-precipitation method. *Journal of Magnetism and Magnetic Materials*, 322(13), 1720-1726.
- [16] Davoodi, A., & Hashemi, B. (2011). Magnetic properties of Sn-Mg substituted strontium hexaferrite nanoparticles synthesized via coprecipitation method. *Journal of Alloys and Comp* Ghasemi, A., & Morisako, A. (2008). Structural and electromagnetic characteristics of substituted strontium hexaferrite nanoparticles. *Journal of Magnetism and Magnetic Materials*, 320(6), 1167-1172.
- [17] Atif, M., Nadeem, M., Grössinger, R., & Turtelli, R. S. (2011). Studies on the magnetic, magnetostrictive and electrical properties of sol-gel synthesized Zn doped nickel ferrite. *Journal of Alloys and Compounds*, 509(19), 5893-5896.
- [17] Atif, M., Nadeem, M., Grössinger, R., & Turtelli, R. S. (2011). Studies on the magnetic, magnetostrictive and electrical properties of sol-gel synthesized Zn doped nickel ferrite. *Journal of Alloys and Compounds*, 509(18), 5720-5724.

- [18] Kalyane, S., & Pathan, A. N. (2021). *COMBUSTION SYNTHESIZED PHYSICAL PROPERTIES OF SOME NANOCRYSTALLINE SUBSTITUTED SPINEL FERRITES SYSTEMS*. Horizon Books (A Division of Ignited Minds Edutech P Ltd).
- [19] Luo, H., Rai, B. K., Mishra, S. R., Nguyen, V. V., & Liu, J. P. (2012). Physical and magnetic properties of highly aluminum doped strontium ferrite nanoparticles prepared by auto-combustion route. *Journal of Magnetism and Magnetic Materials*, 324(17), 2602-260
- [20] Ashiq, M. N., Asi, A. S., Farooq, S., Najam-ul-Haq, M., & Rehman, S. (2017). Magnetic and electrical properties of M-type nano-strontium hexaferrite prepared by sol-gel combustion method. *Journal of Magnetism and Magnetic Materials*, 444, 426-431.
- [21] Hussain, S., Anis-ur-Rehman, M., Maqsood, A., & Awan, M. S. (2006). The effect of SiO₂ addition on structural, magnetic and electrical properties of strontium hexa-ferrites. *Journal of crystal growth*, 297(2), 403-410.
- [22] Kanagesan, S., Jesurani, S., Velmurugan, R., Prabu, S., & Kalaivani, T. (2012). Magnetic properties of Ni–Co doped barium strontium hexaferrite. *Journal of Materials Science: Materials in Electronics*, 23(8), 1575-1579.
- [23] Nyathani, M., Sriramulu, G., Babu, T. A., Prasad, N. V., Ravinder, D., & Katlakunta, S. (2021). Crystal chemistry, magnetic and dielectric properties of nickel doped strontium ferrites. *Biointerface Res. Appl. Chem.*, 12(1), 929-939.
- [24] Roohani, E., Arabi, H., & Sarhaddi, R. (2018). Influence of nickel substitution on crystal structure and magnetic properties of strontium ferrite preparation via sol-gel auto-combustion route. *International Journal of modern physics B*, 32(01), 1750271.
- [25] Lodhi, M. Y., Khan, M. A., Akhtar, M. N., Warsi, M. F., Mahmood, A., & Ramay, S. M. (2018). Role of Nd-Ni on structural, spectral and dielectric properties of strontium-barium based nano-sized X-type ferrites. *Ceramics International*, 44(3), 2968-2975.
- [26] Chen, Q., Wang, X. Q., & Ge, H. L. (2008). Magnetic properties of Aluminum-Substituted strontium hexaferrite prepared by citrate–nitrite sol–gel technique. *International Journal of Modern Physics B*, 22(20), 3413-3420.

- [27] Chen, Q., Wang, X. Q., & Ge, H. L. (2008). Magnetic properties of Aluminum-Substituted strontium hexaferrite prepared by citrate–nitrite sol–gel technique. *International Journal of Modern Physics B*, 22(20), 3413-3420.
- [28] Waghmare, S. P., Borikar, D. M., & Rewatkar, K. G. (2017). Impact of Al doping on structural and magnetic properties of Co-ferrite. *Materials Today: Proceedings*, 4(11), 11866-11872.
- [29] Litsardakis, G., Manolakis, I., Serletis, C., & Efthimiadis, K. G. (2007). Effects of Gd substitution on the structural and magnetic properties of strontium hexaferrites. *Journal of magnetism and magnetic materials*, 316(2), 170-173.
- [30] Shekhawat, D., & Roy, P. K. (2019). Effect of cobalt substitution on physical & electro-magnetic properties of SrAl₄Fe₈O₁₉ hexa-ferrite. *Materials Chemistry and Physics*, 229, 183-189.
- [31] Qiao, L., You, L., Zheng, J., Jiang, L., & Sheng, J. (2007). The magnetic properties of strontium hexaferrites with La–Cu substitution prepared by SHS method. *Journal of magnetism and magnetic materials*, 318(1-2), 74-78.
- [32] Kikuchi, T., Nakamura, T., Yamasaki, T., Nakanishi, M., Fujii, T., Takada, J., & Ikeda, Y. (2010). Magnetic properties of La–Co substituted M-type strontium hexaferrites prepared by polymerizable complex method. *Journal of magnetism and magnetic materials*, 322(16), 2381-2388.
- [33] Asghar, G., & Anis-ur-Rehman, M. (2012). Structural, dielectric and magnetic properties of Cr–Zn doped strontium hexa-ferrites for high frequency applications. *Journal of alloys and compounds*, 526, 85-90.
- [34] Ashiq, M. N., Qureshi, R. B., Malana, M. A., & Ehsan, M. F. (2014). Synthesis, structural, magnetic and dielectric properties of zirconium copper doped M-type calcium strontium hexaferrites. *Journal of alloys and compounds*, 617, 437-443.
- [35] Biswas, A., Bayer, I. S., Biris, A. S., Wang, T., Dervishi, E., & Faupel, F. (2012). Advances in top–down and bottom–up surface nanofabrication: Techniques, applications & future prospects. *Advances in colloid and interface science*, 170(1-2), 2-27.

- [36] Kavgic, M., Mavrogianni, A., Mumovic, D., Summerfield, A., Stevanovic, Z., & Djurovic-Petrovic, M. (2010). A review of bottom-up building stock models for energy consumption in the residential sector. *Building and environment*, 45(7), 1683-1697.
- [37] McFarland, J. R., Reilly, J. M., & Herzog, H. J. (2004). Representing energy technologies in top-down economic models using bottom-up information. *Energy Economics*, 26(4), 685-707.
- [38] Bokov, D., Jalil, A. T., Chupradit, S., Suksatan, W., Ansari, M. J., Shewael, I. H., ... & Kianfar, E. (2021). *Nanomaterial by Sol-Gel Method: Synthesis and Application*.
- [39] Livage, J., Sanchez, C., Henry, M., & Doeuff, S. (1989). The chemistry of the sol-gel process. *Solid state ionics*, 32, 633-638.
- [40] Schmidt, A. H. (1988). Chemistry of material preparation by the sol-gel process. *Journal of Non-Crystalline Solids*, 100(1-3), 51-64.
- [41] Kumar, P. S., Pavithra, K. G., & Naushad, M. (2019). Characterization techniques for nanomaterials. In *Nanomaterials for solar cell applications* (pp. 97-124). Elsevier.
- [42] Holder, C. F., & Schaak, R. E. (2019). Tutorial on powder X-ray diffraction for characterizing nanoscale materials. *ACS Nano*, 13(7), 7359-7365.
- [43] Jain, R. (2022). A Review on the Development of XRD in Ferrite Nanoparticles. *Journal of Superconductivity and Novel Magnetism*, 1-15.
- [44] Nethala, G. P., Tadi, R., Gajula, G. R., Kumar, K. C., & Veeraiah, V. (2018). Investigations on the structural, magnetic and mossbauer properties of cerium doped strontium ferrite. *Physica B: Condensed Matter*, 550, 136-144.
- [45] Augustin, C. O., Selvan, R. K., Nagaraj, R., & Berchmans, L. J. (2005). Effect of La³⁺ substitution on the structural, electrical and electrochemical properties of strontium ferrite by citrate combustion method. *Materials chemistry and physics*, 89(2-3), 406-411.
- [46] Pradeep, A., & Chandrasekaran, G. (2006). FTIR study of Ni, Cu and Zn substituted nano-particles of MgFe₂O₄. *Materials Letters*, 60(3), 371-374.

- [47] Venkatesh, M. S., & Raghavan, G. S. V. (2005). An overview of dielectric properties measuring techniques. *Canadian biosystems engineering*, 47(7), 15-30.
- [48] Van Uitert, L. G. (1956). Dielectric properties of and conductivity in ferrites. *Proceedings of the IRE*, 44(10), 1294-1303.
- [49] Hao, T., Kawai, A., & Ikazaki, F. (2001). Direct differentiation of the types of polarization responsible for the electro rheological effect by a dielectric method. *Journal of colloid and interface science*, 239(1), 106-112.
- [50] Dakin, T. W. (2006). Conduction and polarization mechanisms and trends in dielectric. *IEEE Electric Foner*, S. (1996). The vibrating sample magnetometer: Experiences of a volunteer. *Journal of applied physics*, 79(8), 4740-4745. *al Insulation Magazine*, 22(5), 11-28.
- [51] El-Alaily, T. M., El-Nimr, M. K., Saafan, S. A., Kamel, M. M., Meaz, T. M., & Assar, S. T. (2015). Construction and calibration of a low cost and fully automated vibrating sample magnetometer. *Journal of Magnetism and Magnetic Materials*, 386, 25-30.